Author/s:
Sayers, CP;Mollard, V;Buchanan, HD;McFadden, GI;Goodman, CD

Title:
A genetic screen in rodent malaria parasites identifies five new apicoplast putative membrane transporters, one of which is essential in human malaria parasites

Date:
2018-01-01

Citation:
Sayers, C. P., Mollard, V., Buchanan, H. D., McFadden, G. I. & Goodman, C. D. (2018). A genetic screen in rodent malaria parasites identifies five new apicoplast putative membrane transporters, one of which is essential in human malaria parasites. Cellular Microbiology, 20 (1), https://doi.org/10.1111/cmi.12789.

Sayers Claire (Orcid ID: 0000-0001-7103-4222)

## Title

A genetic screen in rodent malaria parasites identifies five new apicoplast putative membrane transporters, one of which is essential in human malaria parasites

## Authors

Claire P. Sayers[1], Vanessa Mollard, Hayley D. Buchanan, Geoffrey I. McFadden[*], Christopher D. Goodman[*]

[*]These authors contributed equally

[1]Current address: Wellcome Trust Sanger Institute, Wellcome Genome Campus, Hinxton, Cambridgeshire, UK

## Address

School of BioSciences, University of Melbourne, Parkville, Victoria, Australia

## Keywords

Genetic screen; *Plasmodium*; apicoplast; membrane transporter; knockout (KO); knockdown; localise; isopentenyl diphosphate (IPP)

## Summary



This is the author manuscript accepted for publication and has undergone full peer review but has not been through the copyediting, typesetting, pagination and proofreading process, which may lead to differences between this version and the Version of Record. Please cite this article as doi: 10.1111/cmi.12789

The malaria-causing parasite, *Plasmodium*, contains a unique non-photosynthetic plastid known as the apicoplast. The apicoplast is an essential organelle bound by four membranes. Although membrane transporters are attractive drug targets, only two transporters have been characterised in the malaria parasite apicoplast membranes. We selected 27 candidate apicoplast membrane proteins, 20 of which are annotated as putative membrane transporters, and performed a genetic screen in *P. berghei* to determine blood stage essentiality and subcellular localisation. Eight apparently essential blood stage genes were identified, three of which were apicoplast-localised: *Pb*ANKA_0614600 (DMT2), *Pb*ANKA_0401200 (ABCB4) and *Pb*ANKA_0505500. Nineteen candidates could be deleted at the blood stage, four of which were apicoplast-localised. Interestingly, three apicoplast-localised candidates lack a canonical apicoplast targeting signal but do contain conserved N-terminal tyrosines with likely roles in targeting. An inducible knockdown of an essential apicoplast putative membrane transporter, *Pf*DMT2, was only viable when supplemented with isopentenyl diphosphate (IPP). Knockdown of *Pf*DMT2 resulted in loss of the apicoplast, identifying *Pf*DMT2 as a crucial apicoplast putative membrane transporter and a candidate for therapeutic intervention.

## Introduction

Membrane transporters are ideal malaria drug targets as the *Plasmodium* parasite is typically reliant on them to establish an infection within host cells, scavenge from the environment, and shuffle resources between intracellular compartments. Many

membrane transporters are vulnerable to pharmacological agents and used in the treatment of human disease (Kirk, 2004; Kirk & Lehane, 2014). Furthermore, a number of *Plasmodium* transporters are attractive molecular targets for drug design, particularly the hexose transporter (Joët & Krishna, 2004; Joët et al., 2003; Krishna et al., 2000; Woodrow et al., 1999). More recently, both *Pf*ATP4 and *Pf*FNT have emerged as promising drug targets (Rottmann et al., 2010; Spillman et al., 2013; Lehane et al., 2014; Marchetti et al., 2015; Golldack et al., 2017). The *Plasmodium* transportome is a vital area of research that will aid our general understanding of malaria parasite biology, and ultimately offer novel drug targets to fight the disease.

Detailed sequence analysis identified over 100 membrane transport proteins in the *P. falciparum* genome (Martin et al., 2005; Martin et al., 2009). These putative membrane transporters contain multiple hydrophobic transmembrane domains (TMDs) connected by hydrophilic loops, with many having eight to 14 TMDs (Martin et al., 2009). Although this analysis substantially expanded the list of *Plasmodium* transporters, the malaria parasite genome is still considered to be minimalistic in terms of transporter abundance, with just over 2% of the genome encoding transport proteins (Martin et al., 2005). This should therefore result in a low level of redundancy amongst *Plasmodium* transporters relative to the transportomes of other organisms (Martin et al., 2005).

Kenthirapalan et al. (2016) reported a genetic screen of 35 putative membrane transporters in *P. berghei*. During the disease causing blood stage of infection, 17.14% of these putative membrane transporters were found to have essential functions, 11.43% were required for normal growth, and 71.43% could be deleted with no growth defect or arrest across the life cycle (Kenthirapalan et al., 2016). However, of the genes that could be deleted in the blood stage, 45% were found essential for completion of the life cycle, 31% were later required for normal growth and only 24% were not needed for normal growth throughout the entire life cycle (Kenthirapalan et al., 2016). More recently, Bushell et al. (2017) found that of the 79 transporters targeted for genetic deletion in blood stage *P. berghei* parasites, 33% were essential, 24% were necessary for normal growth and 43% were dispensable. This may indicate that many membrane transporters have vital roles beyond the blood stage. Subcellular co-localisations were not provided in these studies, making it difficult to link any deletion effects with possible function within the cell.

A primary feature in eukaryotic cells is the compartmentalisation of function into various membrane bound organelles with different internal environments. Membrane transporters are essential for the function and maintenance of organelles as they regulate the movement of molecules across otherwise impermeable membranes. One of the most intriguing organelles in *Plasmodium* is the apicoplast (McFadden et al., 1996). Derived from an algal chloroplast, the apicoplast contains many bacterial and plant-like pathways that are attractive drug targets because they differ markedly from

pathways found in humans (McFadden & van Dooren, 2004; Ralph et al., 2004). In the red blood cell stages, the only essential function of the apicoplast is the production of isopentenyl diphosphate (IPP) (Yeh & DeRisi, 2011). In *in vitro* culture, genes essential for apicoplast function, and even the entire apicoplast, can be deleted as long as the parasites are provided with a source of IPP (Gisselberg et al., 2013; Yeh & DeRisi, 2011). This is not true for the mosquito and liver stages of the parasite life cycle, where other apicoplast metabolic pathways are essential (Ke et al., 2014; Nagaraj et al., 2013; van Schaijk et al., 2014; Yu et al., 2008; Rathnapala et al., 2017).

To maintain apicoplast metabolism, and thus ensure parasite survival, one or more of the apicoplast membranes must act as a selective molecular barrier. Canonical plant plastids (chloroplasts) have two membranes. The inner membrane contains a number of active transporters, and the outer membrane contains selective channels (Bölter & Soll, 2001; Fischer, 2011; Pick & Weber, 2014). Four membranes surround the apicoplast as a result of its secondary endosymbiotic origins (Köhler et al., 1997; van Dooren & Striepen, 2013). The outer apicoplast membrane is intermittently continuous with the parasite endomembrane system, and the second outermost 'periplastid' membrane is derived from the red algal plasma membrane (van Dooren & Striepen, 2013). The two innermost membranes of the apicoplast are homologous to the two membranes of the primary plastids of red algae and plants (McFadden & van Dooren, 2004; van Dooren & Striepen, 2013). Little is known about the distribution of membrane transport processes across these four membranes and how

apicoplast transporters interact to import molecules required to fuel apicoplast metabolism and export metabolites to the rest of the parasite.

Mullin et al. (2006) characterised the first apicoplast membrane transporters, the inner and outer triose phosphate transporters, *Pf*iTPT and *Pf*oTPT, which are homologs of plant plastidic phosphate translocators (pPTs) (Weber & Linka, 2011). A bipartite leader sequence targets *Pf*iTPT to the innermost apicoplast membrane, whereas *Pf*oTPT, which lacks a targeting leader, localises to the outermost apicoplast membrane (Mullin et al., 2006). The pPTs of *Plasmodium* were later found to fuel apicoplast metabolism by importing phosphoenolpyruvate (PEP), dihydroxyacetone (DHAP) and 3-phosphoglycerate (3PGA) from parasite glycolysis in the cytosol (Brooks et al., 2010; Lim et al., 2010). Banerjee et al. (2012) reported that during the blood stage of infection of the rodent malaria parasite, *P. berghei*, *Pb*oTPT was essential and *Pb*iTPT was dispensable. However, *Pb*iTPT KO parasites displayed growth defects in the mosquito and liver stages (Banerjee et al., 2012). It was suggested that *Pb*oTPT can transport the *Pb*iTPT substrate in blood stage parasites and that the two transporters might not work in tandem (Banerjee et al., 2012). To date, the TPTs remain the only membrane transporters known to be localised to the apicoplast.

Here, we describe a medium throughput genetic screen for apicoplast membrane transporters in *P. berghei*. Candidate apicoplast membrane proteins, many of which

are putative membrane transporters, were identified and then investigated using the *Plasmo*GEM vectors (Gomes et al., 2015; Pfander et al., 2012; Pfander et al., 2011; Schwach et al., 2015). In *P. berghei*, we localised these candidates by gene tagging and determined essentiality in the blood stage by gene knockout (KO) attempts. Gene knockdowns were performed for two apparently essential apicoplast putative membrane transporters in *P. falciparum*, and IPP supplementation was used to investigate the roles of one in apicoplast biogenesis.

## Results

### Candidate apicoplast membrane transporters

We compiled a list of potential *Plasmodium* apicoplast membrane transporters (Table 1) from two sources: *P. falciparum* putative membrane transporters belonging to known transport families (Martin et al., 2005) and selected members of the predicted *P. falciparum* apicoplast proteome with multiple TMDs (Ralph et al., 2004). Many *P. falciparum* membrane transporters have seven or more TMDs, whilst some have six or fewer (Martin et al., 2005). Without biological data to confirm membrane transport activity, we selected candidate proteins predicted to have at least six TMDs (Table 1). Although multiple TMDs is a minimum requirement of most membrane transporters, some of these proteins may be integral membrane proteins with other functions, in which case further investigation is required.

The first 10 candidates in Table 1 are predicted to be apicoplast-localised; the remaining 17 apparently lack apicoplast targeting signals but were included in the hope of extending the list of non-canonically targeted apicoplast membrane transporters. All shortlisted candidates are predicted to contain at least six and up to 17 TMDs, and have orthologues in both *P. berghei* and *P. falciparum* (Table 1). Additionally, nine have *Toxoplasma gondii* orthologues, eight have orthologues in *Theileria*, six in *Babesia* and 10 in *Cryptosporidium* (Table 1). Those with orthologues in *Cryptosporidium*, a model apicomplexan species that lacks an apicoplast (Zhu et al., 2000), were deprioritised. As a final criterion, we considered the level of blood stage expression of each candidate, namely from very low to very high (Table 1). Shortlisting led us to include 27 candidate proteins, 20 of which are putative membrane transporters and 7 of which are putative integral membrane proteins, not currently annotated as transporters (Table 1).

**Blood stage essentiality in rodent malaria**

Initially, our genetic screen aimed to determine whether candidates were essential (parasites refractory to deletion) or non-essential (parasites survive deletion) during the blood stage of infection. This was achieved by attempting to delete candidate genes in *P. berghei*. Parasite lines were generated for 25 gene KO attempts, and PCR screening was performed to determine whether parasites lack the gene of interest or retain the wild-type (WT) locus (Figure 1A; Supplementary figure 1). Nineteen candidates appeared to have successful integration of the KO vector, indicating that

the genes of interest had been deleted (Figure 1A; Supplementary figure 1). These 19 genes were considered to be non-essential for parasite survival at the blood stage. Six candidates were apparently essential for parasite survival at the blood stage as no PCR products detected integration of the KO construct (Figure 1A). Instead, PCR screening generally showed that these parasites retained only the WT locus, suggesting that random integration had occurred and that the gene could not be deleted in surviving parasites (Figure 1A; Supplementary figure 1). Only deletion of *Pb*ANKA_0505500 yielded no parasites after three transfections with a KO construct. Therefore, *Pb*ANKA_0505500 was deemed probably essential at the blood stage but PCRs could not be included in Figure 1A (Table 1).

We analysed a subset of the generated parasite lines, using Southern blotting to validate our genetic screen results. This confirmed our PCR results showing that *Pb*ANKA_0614600 and *Pb*ANKA_0942100 are probably essential (Supplementary figures 2-4). Additionally, the candidate apicoplast membrane transporter, *Pb*ANKA_0401200, was reported to be refractory to deletion by Rijpma et al. (2016). We recovered parasites from only one of three transfections with the *Pb*ANKA_0401200 KO construct, and while our PCR results indicated that integration had occurred (Supplementary figure 1), we set out to validate our positive result by Southern blot (Supplementary figures 5-6). The results of the Southern blot were unclear for integration of the KO construct (Supplementary figure 6) so mRNA expression was examined by reverse transcriptase (RT)-PCR (Figure 1B-C). Three

primer pairs within the *Pb*ANKA_0401200 coding sequence amplified the expected WT product sizes from parasites carrying the *Pb*ANKA_0401200 KO construct (Figure 1B-C). This suggested that an unusual integration occurred in *Pb*ANKA_0401200 KO parasites, where the gene locus was modified but the gene is still expressed. We thus suggest that *Pb*ANKA_0401200 is essential at the blood stage.

*Plasmo*GEM transfection vectors are expected to have low rates of random integration and episomally maintained vectors (Pfander et al., 2011). However, in our experimental system, growth of parasites retaining the WT locus was common, indicating that many *Plasmo*GEM KO vectors can experience some random integration.

**Protein expression and apicoplast localisation**

Sixteen candidate genes were HA-tagged for localisation experiments in *P. berghei*. PCR screening confirmed that all parasite lines contain the HA-tag (TAG) vector (Supplementary figure 7) and expression of the tagged protein was confirmed by Western blot (Figure 2A). Thirteen candidates had bands of the appropriate mass congruent with gene models (Figure 2A), and three (*Pb*ANKA_0942100, *Pb*ANKA_0410500 and *Pb*ANKA_0916000) likely suffer from electrophoresis anomalies common to membrane proteins (Kaur & Bachhawat, 2009). *Pb*ANKA_0809500 TAG protein could not be detected in blood stage parasites (data

not shown), which have low expression of the gene (Table 1), so protein was extracted from sporozoite parasites where expression was higher. Particularly faint signal was observed for *Pb*ANKA_0417100 (Figure 2A), which is lowly expressed during the blood stages (Table 1). Tagged parasite lines were also generated in *P. falciparum*. *Pf*3D7_1145500-GFP (*Pb*ANKA_0903500 orthologue) had two GFP bands that were smaller than the predicted mass; the smallest may be dissociated GFP (Figure 2B). Finally, *Pf*3D7_0716900-*glmS* (*Pf*DMT2-*glmS*), *Pf*3D7_0302600-*glmS* (*Pf*ABCB4-*glmS*) and *Pf*3D7_0302600-HA (*Pf*ABCB4-HA) had HA bands at the predicted masses (Figure 2C; Supplementary figure 8).

Immunofluorescence assays (IFAs) were performed for all tagged candidate genes. Seven candidates co-localised with the apicoplast marker, ACP (Figure 3A-B). *Pb*ANKA_0809500, *Pb*ANKA_0401200, *Pb*ANKA_0505500 and *Pf*3D7_1145500 were all predicted to have apicoplast targeting leader sequences whilst *Pb*ANKA_1103600, *Pb*ANKA_1304700 and *Pf*DMT2 were not predicted to contain leader sequences (Figure 3A-B; Table 1). Another seven candidates localised to non-apicoplast structures within the parasite (Figure 3D). Four candidates had no observable immunofluorescence signal at the blood stage so could not be localised in this life cycle stage: *Pb*ANKA_0942100, *Pb*ANKA_0417100, *Pb*ANKA_1446100 and *Pb*ANKA_0602400 (data not shown). Life cycle analysis of two candidates (*Pb*ANKA_1103600 and *Pb*ANKA_0942100) revealed that *Pb*ANKA_1103600 TAG was expressed and localised to the apicoplast in midgut oocysts, salivary gland

sporozoites and *in vitro* liver cell stage parasites (Figure 3C). No signal was observed for *Pb*ANKA_0942100 TAG parasites at any life cycle stage so its localisation remains unknown (data not shown).

The results of the screen are summarised in Figure 4, highlighting the essentiality of the candidates and whether they are localised to the apicoplast. The characteristics of each candidate gene are represented in Table 1 by colour-coded categories based on their location in the Venn diagram (Figure 4).

**Knockdown of essential apicoplast putative membrane transporters in human malaria**

Two candidates, identified as blood stage essential in the *P. berghei* genetic screen (*Pb*ANKA_0401200 and *Pb*ANKA_0614600: *Pb*ABCB4 and *Pb*DMT2 respectively), were followed up with conditional knockdowns of orthologues in the human malaria parasite, *P. falciparum* (*Pf*3D7_0302600 and *Pf*3D7_0716900: *Pf*ABCB4 and *Pf*DMT2 respectively). Glucosamine (GlcN)-induced *glmS* ribozyme knockdowns (Prommana et al., 2013) were generated and clonal integrant, WR99210 (WR)-resistant, parasites were obtained (Figure 5; Supplementary figure 9). The highest concentration of GlcN that allowed normal growth of the WT 3D7 parental line and a line carrying an HA-tagged protein targeted to the apicoplast (*Pf*ABCB4-HA) is 2.5 mM GlcN (Supplementary figure 10), so this concentration was selected for knockdown of transcripts in the *glmS* lines.

Localisation of *Pf*DMT2-*glmS*, *Pf*ABCB4-*glmS* and *Pf*ABCB4-HA confirmed the predicted apicoplast localisations and that the HA-tag and *glmS* additions do not interfere with targeting (Figure 3A). Western blot analysis of *Pf*DMT2-*glmS* parasites grown with and without GlcN confirmed an efficient knockdown of the putative transporter (Figure 2C-E). This knockdown trend was also observed in a different clonal line of *Pf*DMT2-*glmS* parasites (Supplementary figure 11). It is noteworthy that expression of *Pf*DMT2-*glmS* (without the addition of GlcN) fluctuates across the asexual cycle, with lowest expression in the merozoite/ring stage (0, 48 and 96 hours) (Figure 2C). Nevertheless, addition of GlcN dramatically reduces the amount of *Pf*DMT2 protein (Figure 2D-E; Supplementary figure 11). In contrast, the addition of GlcN to *Pf*ABCB4-*glmS* parasites did not substantially reduce protein levels, nor did it impede growth (Supplementary figure 10; Supplementary figure 12). Therefore, it was not possible to conclude if *Pf*ABCB4 is essential at the blood stage.

**_Pf_DMT2 knockdown is lethal but can be rescued with IPP supplementation**

*Pf*DMT2-*glmS* parasites were grown with different combinations of 2.5 mM GlcN and/or 200 µM IPP to determine whether *Pf*DMT2 knockdown abrogates growth and whether a growth phenotype can be rescued by supplying exogenous IPP (Figure 6). As expected, IPP alone had no effect on the growth or morphology of *Pf*DMT2-*glmS* parasites in a six-day growth trial (Figure 6). Addition of GlcN to control parasites with IPP supplementation also had no effect on growth (Figure 6). In contrast,

different clonal lines of *Pf*DMT2-*glmS* parasites exposed to GlcN replicated normally in the first 48 hours but then failed to grow thereafter, with few healthy parasites visible after six days (Figure 6; Supplementary figure 13A-B). Growth of these knockdown parasites was restored when supplemented with IPP (Figure 6; Supplementary figure 13A-B), suggesting an apicoplast specific function for *Pf*DMT2. Western blot analysis confirmed that *Pf*DMT2 protein expression was knocked down in these IPP rescued parasites (Supplementary figure 13C-D).

The effects of GlcN treatment are reversible as long as parasites remain viable (Prommana et al., 2013). *Pf*DMT2 knockdown parasites could recover when GlcN was removed after 12 days of treatment (Supplementary figure 13). In contrast, IPP rescued knockdown parasites could not be recovered when GlcN and IPP were removed (Figure 6; Supplementary figure 13A-B), suggesting that the apicoplast was irreversibly compromised in *Pf*DMT2 knockdown parasites rescued with IPP. It should also be noted that with prolonged exposure to GlcN, a small subpopulation of knockdown parasites became insensitive to the treatment. Parasites could be recovered after 14 days in culture with GlcN, after which *Pf*DMT2 expression was detected (Supplementary figure 13).

**Rescued *Pf*DMT2 knockdown parasites are apicoplast-minus**

To test whether knocking down *Pf*DMT2 resulted in loss of the apicoplast, we used real-time quantitative PCR to assess the impact of the *Pf*DMT2 knockdown on the

apicoplast genome (Figure 7). By assessing the ratio of a single copy apicoplast gene to a single copy nuclear gene, and including a mitochondrial gene as a control, we measured the impact of GlcN and IPP on the apicoplast of *Pf*DMT2-*glmS* parasites across three 48-hour red blood cell life cycles (Figure 7). In absence of IPP and GlcN, both *Pf*DMT2-*glmS* and control parasites retain the apicoplast genome (Figure 7). In contrast, in *Pf*DMT2-*glmS* parasites exposed to GlcN but rescued with IPP, there was no evidence of the apicoplast genome after three or six 48-hour life cycles (Figure 7; Supplementary figure 14). Apicoplast loss in these parasites was confirmed by IFA with no defined apicoplast structure visible in *Pf*DMT2-*glmS* parasites treated with IPP and GlcN (Supplementary figure 15).

## Discussion

Membrane transporters have good drug target potential (Kirk, 2004; Krishna et al., 2001; Kirk & Lehane, 2014) so the *Plasmodium* transportome is a vital area of malaria research (Krishna et al., 2001; Kirk & Lehane, 2014). However, there is a lack of biological data for membrane transporters in *Plasmodium*, particularly for those on intracellular membranes (Kirk, 2004; Krishna et al., 2001; Kirk & Lehane, 2014). Only two apicoplast membrane transporters have been characterised to date (Mullin et al., 2006). It continues to be crucial to understand how molecules pass across the apicoplast membranes to fully understand *Plasmodium* biology and potentially offer novel drug targets. We set out to expand our understanding of apicoplast membrane transporters and their potential as drug targets by undertaking a

medium throughput genetic screen addressing two central questions: *which proteins are essential for parasite survival at the blood stage*, and *which are localised to the apicoplast?*

Five putative membrane transporters and three putative integral membrane proteins were identified as apparently essential at the *P. berghei* blood stage, flagging them as potentially good drug targets worthy of further characterisation. Two of these putative membrane transporters, *Pb*ANKA_0614600 (DMT2) and *Pb*ANKA_0401200 (ABCB4), and one of the putative integral membrane proteins, *Pb*ANKA_0505500, were apicoplast-localised. *Pf*DMT2 is a putative drug/metabolite transporter. Knockdown of *Pf*DMT2 prevents parasites from replicating in the second cycle; a phenotype reminiscent of the 'delayed death' response to apicoplast targeting drugs described in *Plasmodium* and other apicomplexan parasites (Fichera et al., 1995; Goodman et al., 2007). Parasites treated with delayed death drugs can be rescued in culture by the addition of IPP, the only essential metabolic product of the apicoplast during the red blood cell stage (Yeh & DeRisi, 2011). Here, we showed that the lethality of the *Pf*DMT2 knockdown phenotype is completely reversed by addition of IPP. This allowed us to conclude that abatement of *Pf*DMT2 disrupts apicoplast function, as confirmed by absence of the apicoplast genome and lack of a microscopically identifiable apicoplast organelle in knockdown parasites rescued with IPP supplementation. Unfortunately, an efficient knockdown of *Pf*ABCB4 could not be achieved with our system. This appears to be one of the limitations of this

inducible knockdown strategy and highlights the importance of trialing a number of different approaches to disrupt an essential candidate gene. The knockdown phenotype of *Pb*ANKA_0505500 remains to be tested.

Based on phylogenetic data showing the absence of a DMT2 orthologue in *Cryptosporidium* and the localisation of *Pb*DMT2 to an unknown intracellular structure (Kenthirapalan et al., 2016), Weiner 3rd & Kooij (2016) proposed that DMT2 might be an apicoplast-localised transport protein perhaps involved in IPP transport or the import of iron or sulfur for the iron-sulfur cluster biosynthesis pathway. Our analysis suggests that *Pf*DMT2 has a function in apicoplast maintenance rather than being solely an IPP transporter. Treatment of parasites with drugs disrupting housekeeping functions under IPP supplementation results in apicoplast loss (Yeh & DeRisi, 2011), while disruption of apicoplast IPP synthesis with IPP supplementation leaves the apicoplast intact (Gisselberg et al., 2013). By extension, disrupting an apicoplast housekeeping transporter while rescuing it with IPP should result in loss of the apicoplast through lack of a crucial biogenesis function. Conversely, the apicoplast should remain intact under IPP supplementation if the only role of the protein knocked down is IPP export. This assumes that a block in IPP export, and a consequent accumulation of IPP, is not toxic. If IPP build up is toxic, disrupting an IPP exporter could result in a similar phenotype to targeting an apicoplast housekeeping gene. Our initial finding that *Pf*DMT2 is essential for the maintenance of the apicoplast shows that *Pf*DMT2 may not exclusively be an IPP

exporter, but likely plays a different, and/or additional role in apicoplast function. It would be premature to totally dismiss *Pf*DMT2 as a candidate IPP transporter that also has other roles in apicoplast metabolism, but further work is clearly required to confirm its biological role.

One important consideration when screening for *Plasmodium* apicoplast membrane transporters is the potential exclusion of candidates based on the absence of predicted targeting motifs. Current prediction tools (Foth et al., 2003; Zuegge et al., 2001) are designed to predict the probability of a *P. falciparum* protein containing a canonical bipartite leader sequence. *Pf*oTPT, one of the first apicoplast membrane transporters characterised and localised to the outer membrane, does not contain a leader (Mullin et al., 2006) and was not predicted to be apicoplast-localised. The targeting information required for the correct localisation of this type of membrane protein remains largely unexplored, in part because of a lack of confirmed, leaderless proteins to include in analyses. The only confirmed targeting information for these leaderless proteins is the presence of a tyrosine in the N-terminal region of the *Toxoplasma* orthologue of oTPT (DeRocher et al., 2012), and we recently established that an N-terminal tyrosine residue is necessary but not sufficient for the apicoplast targeting of *Pf*oTPT (Lim et al., 2016).

A number of leaderless candidate membrane proteins were included in our genetic screen with the hope of identifying further leaderless apicoplast membrane

transporters. This proved successful with the identification of three novel leaderless apicoplast putative membrane transporters: DMT2, *Pb*ANKA_1103600 (ATP3) and *Pb*ANKA_1304700 (MFS6). Intriguingly, protein alignments revealed that these novel leaderless apicoplast proteins contain conserved N-terminal tyrosines just upstream of, or within the first TMD (Supplementary figure 16). These proteins provide a starting point for dissecting the process of leaderless apicoplast targeting by determining the universality of the N-terminal tyrosine in apicoplast targeting and whether it is outer membrane specific.

In addition to the blood stage essential candidates identified here, we found 18 candidates to be non-essential for blood stage growth. Furthermore, Rijpma et al. (2016) determined that our candidate *Pb*ANKA_0903500 (ABCB3) is not essential at the blood stage. Together, 70% of our candidate proteins could be deleted in blood stage *P. berghei* parasites. Although termed non-essential in this study, it is important to consider that parasite fitness was not measured so a number of these candidates may be required for normal growth and become essential when in competition with other parasites in the field. Four of these 19 non-essential candidates were apicoplast-localised in this study: three putative membrane transporters (ABCB3, ATP3 and MFS6), and one putative integral membrane protein (*Pb*ANKA_0809500). Our blood stage essentiality results are largely consistent with recent findings (Kenthirapalan et al., 2016; Rijpma et al., 2016; Bushell et al., 2017) and combining these gives a broader understanding of the make-up of the putative parasite and apicoplast

transportomes. It is becoming apparent that a number of *Plasmodium* putative membrane transporters can be deleted in blood stage parasites, shifting focus to the essential roles of membrane transporters during the mosquito and liver stages.

Interestingly, there are some differences in our combined *Plasmodium* transportome essentiality data. *Pb*ANKA_1364800 (ABCB6) was found to be essential at the blood stage when Rijpma et al. (2016) could not generate ABCB6 KO parasites in *P. berghei* or *P. falciparum*, and Bushell et al. (2017) deemed *Pb*ABCB6 probably essential for blood stage growth. This is contrary to our results, where we deleted *Pb*ABCB6 in blood stage parasites. Further, we were unable to detect integrated *Pb*ANKA_0107700 (ZIP1) KO blood stage parasites and deemed it probably essential. In contrast, Kenthirapalan et al. (2016) generated ZIP1 KO blood stage parasites that had a growth defect and could not infect mosquitos. Later experiments also generated *Pb*ZIP1 KO parasites that grew significantly slower during the blood stage (Bushell et al., 2017). Bushell et al. (2017) reported several other contrasting results that *Pb*ANKA_1429300 and *Pb*ABCB4 are dispensable, and *Pb*ATP3 and *Pb*ANKA_1446100 are essential for blood stage growth.

It is noteworthy that the recovery of KO parasites may depend on the mutagenesis system used and that growth defects can have different impacts depending on the assays used. Rijpma et al. (2016) also reported that *Pb*ABCB3 KO parasites had a severe blood stage growth defect whilst *Pf*ABCB3 KO parasites had no growth defect

in asexual blood stage or mosquito stage parasites. The conflicting reports between *P. berghei* and *P. falciparum* ABCB3 orthologues are a reminder that although these species are often considered somewhat equivalent, they are different and require independent validation to determine whether a gene has the same role in both organisms.

It is important to consider blood stage redundancy before embarking on any targeted drug development strategy. The parasite undergoes remarkable morphological changes during its life cycle (Hall et al., 2005) so it should not be surprising that transportome proteins are switched on and off as the parasite changes between diverse host environments. It is vital to distinguish between membrane transporters that are essential for parasite growth at some stage (growth arrest phenotype) and membrane transporters that are likely redundant and completely dispensable (no growth phenotype at any stage). Life cycle studies will hopefully address the question of whether blood stage dispensable genes are essential elsewhere. Genes essential in pre-erythrocytic or transmission stages are ideal candidates for transmission or prophylactic drugs, which are essential in world malaria control efforts to prevent disease spread and ultimately support eradication.

In summary, we have generated biological data for a number of *Plasmodium* putative membrane transporters and integral membrane proteins, including five apicoplast putative membrane transporters and two apicoplast putative integral membrane

proteins. This study has vastly expanded our knowledge of what proteins reside in the apicoplast membranes and boosted the running total to nine membrane proteins (Figure 8). The identification of three novel leaderless apicoplast putative membrane transporters confirms the existence of a cohort of non-canonically targeted apicoplast membrane transporters and should prove useful in the search for novel apicoplast targeting mechanisms and reveal a great deal about apicoplast biology. Heterologous expression and transport assays will be vital in confirming any transporter roles and determining any substrate specificities of the three new apparently blood stage essential apicoplast putative membrane transporters identified here, one of which is not currently predicted to be a transporter. Defining the function of *Pf*DMT2 in the apicoplast will be a major new insight. The *Plasmodium* apicoplast continues to be an attractive drug target that is unique from its mammalian host. While there is still a lot to learn about the *Plasmodium* transportome, this work provides a platform for future studies to achieve a better understanding of apicoplast biology and identify novel molecular targets to treat or prevent malaria.

## Experimental procedures

### Candidate gene selection

Potential *Plasmodium* apicoplast membrane transporters were shortlisted from two lists: 80 *P. falciparum* putative transport proteins (Martin et al., 2005) and 392 predicted *P. falciparum* apicoplast proteins that contain multiple TMDs (Ralph et al., 2004). The lists were screened using the *Plasmodium* genome database (*Plasmo*DB)

version 30 (Aurrecoechea et al., 2009) and protein localisation predictions were performed with *Plasmo*AP (Foth et al., 2003) and PATS (Zuegge et al., 2001). Gene orthologues were obtained for each candidate from OrthoMCL (Li et al., 2003) and TMD predictions were generated by TMHMM version 2.0 (http://www.cbs.dtu.dk/services/TMHMM/) and TMpred (http://www.ch.embnet.org/software/TMPRED_form.html). Candidates with at least one prediction of 6 TMDs were selected. Although some candidate proteins with multiple TMDs may not be membrane transporters, they were included due to the difficulty in definitively predicting membrane protein structure from protein sequence. Finally, *P. berghei* blood stage expression data was obtained for all candidates (Otto et al., 2014) and binned with thresholds on sample percentiles.

**Maintenance of *P. berghei* and *P. falciparum***

All animal procedures and experiments were performed in agreement with the local Prevention of Cruelty to Animals legislation and the University of Melbourne Animal Ethics Committee guidelines under ethics permits 1112043, 1212488 and 1413078. *P. berghei* ANKA (*Pb*ANKA) blood stage parasites were grown in four to six week old Swiss Webster mice that were sourced from the Monash Animal Research Platform. All *P. falciparum* blood stage culturing experiments were performed with human red blood cells (Australian Red Cross Blood Service) and in agreement with the University of Melbourne Human Ethics Committee guidelines under the ethics permit 1647087. *P. falciparum* 3D7 and D10 strain parasites were maintained as previously

described (Trager & Jensen, 1976) in 2% hematocrit in RPMI-Hepes (WEHI) supplemented with Albumax II (Gibco) and sodium bicarbonate.

**Transfection vectors**

Twenty-three KO and 16 HA-tag (TAG) transfection vectors were sourced from *Plasmo*GEM (plasmogem.sanger.ac.uk; Supplementary table 1). Three candidate genes were predicted to be apicoplast-localised and did not have *Plasmo*GEM KO transfection vectors available at the time. Double crossover homologous recombination KO constructs were therefore made for *Pb*ANKA_0942100, *Pb*ANKA_0401200 and *Pb*ANKA_0505500 (Supplementary figure 17A). Typical KO and tagging strategies for all candidates are outlined in Supplementary figure 17. Primers were used to generate homologous 5' and 3' gene specific flanks (Supplementary table 2). The two flanks were ligated into the intermediate pGEM-T Easy Vector (Promega) and sequenced by the Australian Genome Research Facility (AGRF) with 5'-atttaggtgacactatag (SP6) and 5'-taatacgactcactataggg (T7) primers. DNA flanks were ligated into either side of the pLDC (fusion of mCherry to the DHFR in the pL0006 vector (Malaria Research and Reference Reagent Resource Center)) selectable marker, DHFR, with corresponding restriction enzyme sites. Single crossover *glmS* ribozyme knockdown and control HA constructs were then made for *Pf*3D7_0302600 and *Pf*3D7_0716900 (Supplementary figure 18) to HA-tag and induce protein knockdown. The primers used to generate each gene specific flank are in Supplementary table 3. BglII and PstI were used to ligate each flank into *glmS*

and HA transfection vectors (Elsworth et al., 2014). Final plasmid DNA was sequenced by the AGRF with SP6, 5'-agctgccatatccctcgac, 5'-tgcacacaacatacacatttttac, 5'-tgtaaaacgacggccagt (M13-forward) and 5'-tccaatgtgcatgataaaagaaa primers.

**Parasite transfection**

Approximately 10 µg of *P. berghei* DNA was linearised by NotI (*Plasmo*GEM vectors) and EcoRI/HindIII (pLDC vectors), and electroporated into WT *Pb*ANKA schizonts with an Amaxa Nucleofector Device (Lonza), as previously described (Janse et al., 2006). After 24 hours, pyrimethamine (TCI) was added to the mouse drinking water to a final concentration of 70 µg/mL. Mice were typically monitored for pyrimethamine-resistant parasites until day 14 post infection. Candidate genes were considered to be probably essential at the blood stage if mice remained uninfected after 14 days. At least three biological replicates were performed in this case to confirm the negative result. Using the standard transfection protocol (Crabb & Cowman, 1996; Wu et al., 1995), approximately 100 µg of *Pf*3D7_1145500-GFP plasmid DNA (gift from Liting Lim) was electroporated into ring stage WT *P. falciparum* D10 strain parasites and *Pf*3D7_0302600-*glmS*, *Pf*3D7_0302600-HA and *Pf*3D7_0716900-*glmS* plasmid DNA into ring stage WT *P. falciparum* 3D7 strain parasites. On day two, 1 pM/mL WR (Sigma-Aldrich) was added. WR-resistant parasites were recovered after 15 to 30 days. To encourage the plasmid DNA to

integrate into the parasite genome, parasites were cycled off WR twice, for three weeks at a time.

**Parasite genotyping**

In general, clonal parasites were not required in the *P. berghei* screen and mixed parasite populations were analysed. However, a clonal population of *Pb*ANKA_0401200 KO parasites was required for Southern blot and RT-PCR analyses. A clonal line was recovered after diluted parasites were inoculated into 10 naïve mice. Clonal populations of all *P. falciparum* parasite lines were recovered after diluting in 96-well plates. Pyrimethamine-resistant parasite populations were screened with PCR primers detecting the WT locus, successful integration and presence of the transfection vector (Supplementary figure 17; Supplementary tables 4-5). PCR primers also detected the WT locus and successful integration of WR-resistant parasites (Supplementary figure 18; Supplementary table 6). A Southern blot was performed on *Pb*ANKA_0401200 KO clonal parasite and *Pb*ANKA_0942100 KO and *Pb*ANKA_0614600 KO parasite gDNA using the gene specific 5' flank and DHFR sequences as probes. To generate digoxigenin-labelled (Roche) probes, *Pb*ANKA_0942100 and *Pb*ANKA_0401200 utilised the 5' flank cloning primers (Supplementary table 2) and *Pb*ANKA_0614600 used 5' flank primers (5'-gcaatgcgttttgtgcttag and 5'-gcttccaccgcaaatttattc). A standard DHFR probe was also used (Supplementary figure 19). Additionally, RNA was extracted from *Pb*ANKA_0401200 KO clonal parasites for cDNA synthesis with SuperScript III

Reverse Transcriptase (Invitrogen). To determine whether *Pb*ANKA_0401200 was expressed in KO parasites, primers were designed within the coding sequence for RT-PCR (Supplementary table 7).

**Generating pre-erythrocytic stage parasites**

*Pb*ANKA_1103600, *Pb*ANKA_0942100 and *Pb*ANKA_0809500 TAG parasite lines were used to infect approximately 100 naïve female *Anopheles stephensi* strain MR4 mosquitoes. Mosquito midgut oocysts were typically harvested from day 9 post infection and salivary gland sporozoites from day 20 post infection. Furthermore, human hepatoma HepG2 cells (ATCC) were grown (Hollingdale et al., 1983) and infected with *Pb*ANKA_1103600 and *Pb*ANKA_0942100 TAG sporozoites.

**Western blot analysis**

Saponin-isolated intraerythrocytic parasites were resuspended in reducing buffer and heated to 70°C before analysis. For sporozoite protein, approximately 100,000 sporozoites were released from mosquito salivary glands to which reducing buffer was added before freezing. Protein samples were electrophoresed using the NuPAGE system (Thermo Fisher Scientific) and transferred from the gel to a 0.22 µm UltraCruz Nitrocellulose Pure Transfer Membrane (Santa Cruz Biotechnology) or a 0.45 µm polyvinyl difluoride (PVDF) membrane (Thermo Fisher Scientific). After blocking, membranes were incubated with a monoclonal rat anti-HA antibody (1:250; Roche), mouse anti-GFP antibody (1:100; Roche), rat anti-BiP antibody (1:500;

ATCC) or apicoplast marker acyl carrier protein (ACP) anti-serum, rabbit anti-ACP (1:250). After washing, membranes were incubated with goat anti-rat horseradish peroxidase-conjugated (HRP) antibody, goat anti-mouse HRP antibody or goat anti-rabbit HRP antibody (1:1000; Thermo Fisher Scientific). Protein bands were detected with the SuperSignal West Pico Chemiluminescent Substrate (Thermo Fisher Scientific). In addition, *glmS* ribozyme knockdown and HA-tag control parasites were grown with or without GlcN and saponin-isolated at 0, 12, 24, 48, 72, 96 and 120 hours before analysing as above. To normalise Western blot expression data, the ratio of HA to BiP signal was calculated by determining the signal peak area of each lane on the Western blot using the gel analysis tool in Fiji (Schindelin et al., 2012).

**Immunofluorescence assays**

Infected blood, diluted to 1% in RPMI-Hepes with sodium bicarbonate, was adhered to 0.5 mg/mL concanavalin A (conA, Type V; Sigma-Aldrich)-coated 1.5 coverslips (Leica) as described (McMillan et al., 2013). Cells were fixed with 4% paraformaldehyde, 0.005% to 0.0075% glutaraldehyde (Electron Microscopy Sciences) in 1X Dulbecco's Phosphate Buffered Saline (DPBS) for 20 minutes and permeabilised with 0.1% Triton X-100 (Fisher Scientific) in 1X DPBS for 10 minutes. After washing, non-specific labeling caused by glutaraldehyde was reduced by incubating cells in 0.1 mg/mL sodium borohydride (BDH Chemicals) in 1X DPBS for 5 minutes. Cells were washed before blocking in 3% bovine serum albumin (BSA; Sigma-Aldrich) in 1X DPBS. Primary antibodies, monoclonal rat anti-HA, mouse

anti-GFP and rabbit anti-ACP, were incubated with the cells before washing. Secondary antibodies, goat anti-rat Alexa Fluor 488, goat anti-mouse Alexa Fluor 488 and goat anti-rabbit Alexa Fluor 546 (1:5000; Thermo Fisher Scientific), were then added for incubation before washing. Hoechst 33342 (1:10,000; Thermo Fisher Scientific) was included in the first few washes. Cells were mounted with 0.01% DABCO (Sigma-Aldrich) in 50% glycerol and 1X DPBS. The same antibodies were used in the following pre-erythrocytic parasite IFAs.

Infected midguts were fixed in 4% paraformaldehyde in 1X DPBS for 1 hour. Blocking and permeabilisation were performed at 4°C overnight in 0.25% Triton X-100 in 5% BSA. Midguts were incubated with primary antibodies for at least 4 hours with shaking before washing three times with 1X DPBS. Samples were then incubated in secondary antibodies for 2 hours on an orbital shaker and then left at 4°C overnight. Midguts were washed three times with the second wash containing Hoechst. Finally, midguts were mounted with DAKO (Agilent). Sporozoites were added to 3% BSA-coated coverslips and incubated at 37°C for up to 15 minutes. Sporozoites were fixed with 4% paraformaldehyde in 1X DPBS for 10 minutes and permeabilisation was achieved with 0.2% Triton X-100 in 1X DPBS for 20 minutes. Samples were incubated with primary antibodies for at least 1 hour, washed three times and then incubated with secondary antibodies for at least 1 hour. The antibody solution was washed away with one wash containing Hoechst. Again, samples were mounted with DAKO. Finally, infected *in vitro* liver cells were fixed with 4%

paraformaldehyde for 20 minutes at 24, 48 and 63 hours post infection. Cells were washed before 0.1% Triton X-100 in 1X DPBS was added for 20 minutes for permeabilisation. After washing, 3% BSA in 1X DPBS was added for 30 minutes before the liver cell-coated coverslips were placed on the primary antibodies for 1 hour. Coverslips were washed three times before being placed on secondary antibodies containing Hoechst for 1 hour. The coverslips were washed then mounted with DAKO. IFAs were imaged on an inverted Leica SP2 or Nikon A1R confocal microscope with a 63X oil immersion objective. Image brightness, contrast and noise were adjusted in Fiji (Schindelin et al., 2012) when appropriate, and images were merged.

**Protein alignments**

Gene orthologues and protein sequences were obtained from *Plasmo*DB and OrthoMCL (Aurrecoechea et al., 2009; Li et al., 2003) and predicted TMD locations were generated by HMMTOP (Tusnády & Simon, 1998; 2001). Clustal Omega (1.2.2) Multiple Sequence Alignment (Sievers et al., 2011) was used to align gene orthologue protein sequences.

***P. falciparum* growth assays**

The fluorescence-based technique for drug trials in *P. falciparum* was used to determine the effect of GlcN (Sigma-Aldrich) on WT 3D7, ABCB4-HA and ABCB4-*glmS* parasite growth (Smilkstein et al., 2004). Data were normalised to no drug and

no parasite controls before a logarithmic drug curve was plotted with GraphPad Prism version 7.0b. For IPP supplementation, *Pf*DMT2-*glmS* and control parasites were grown in 5 mL cultures for up to 18 days with different treatments of 2.5 mM GlcN and 200 μM IPP (Yeh & DeRisi, 2011). Cultures were smeared every 24 hours, which were imaged with a Leica DM2500 microscope using a 40X objective and a Leica DC300F camera. A Giemsa-Counter plugin in Fiji (Schindelin et al., 2012) was used to count a minimum of 2000 red blood cells per sample. Parasites within the red blood cells were then manually counted to determine parasitaemia. Cultures were subbed to approximately 1% parasitaemia every 48 hours.

**Real-time PCR**

Primers were designed to target genes in the mitochondrial, apicoplast and nuclear genomes (Supplementary table 8), which were used to amplify DNA extracted from IPP supplemented and control parasites. A 2X KAPA SYBR FAST qPCR Master Mix (Universal; Kapa Biosystems) was used for real-time PCR reactions with the following conditions: 95°C (3 minutes, 1 cycle), 95°C (10 seconds), 60.2°C (30 seconds, 40 cycles) and 60 to 95°C (5 seconds, increasing 0.5°C per hold). Every reaction was performed in triplicate and the quantification cycle (Cq) values were obtained for each. The relative quantification of gene expression, or the ratio of organellar to nuclear DNA relative to WT, was then calculated as previously described (Schmittgen & Livak, 2008).

## Acknowledgements

We thank the *Plasmo*GEM team, particularly Ellen Bushell, at the Wellcome Trust Sanger Institute for the majority of the *P. berghei* transfection vectors and Tania de Koning-Ward and Paul Gilson for the *P. falciparum* ribozyme knockdown and control HA-tag transfection vectors. Anton Cozijnsen and Liting Lim are thanked for their technical assistance, and the Australian Red Cross Blood Service is gratefully acknowledged for providing human red blood cells for culturing. Stuart Ralph is thanked for providing his list of putative apicoplast proteins, Lachlan Whitehead is acknowledged for creating the Giesma-Counter plugin for Fiji, and Daniele Muraro is thanked for his assistance with the analysis of published expression data. Claire Sayers was supported by a Melbourne Research Scholarship and the David Lachlan Hay Memorial Fund. This work was funded by an Australian Research Council Discovery Project (DP160104980), and National Health and Medical Research Council Program (637406) and Project (1106213) Grants.

## References

Aurrecoechea, C., Brestelli, J., Brunk, B. P., Dommer, J., Fischer, S., Gajria, B., et al. (2009). *Plasmo*DB: a functional genomic database for malaria parasites. *Nucleic Acids Research*, *37*(Database issue), D539–D543. http://doi.org/10.1093/nar/gkn814

Banerjee, T., Jaijyan, D. K., Surolia, N., Singh, A. P., & Surolia, A. (2012). Apicoplast triose phosphate transporter (TPT) gene knockout is lethal for

*Plasmodium*. *Molecular and Biochemical Parasitology*, *186*(1), 44–50. http://doi.org/10.1016/j.molbiopara.2012.09.008

Bölter, B., & Soll, J. (2001). Ion channels in the outer membranes of chloroplasts and mitochondria: open doors or regulated gates? *The EMBO Journal*, *20*(5), 935–940. http://doi.org/10.1093/emboj/20.5.935

Brooks, C. F., Johnsen, H., van Dooren, G. G., Muthalagi, M., Lin, S. S., Bohne, W., et al. (2010). The *Toxoplasma* apicoplast phosphate translocator links cytosolic and apicoplast metabolism and is essential for parasite survival. *Cell Host and Microbe*, *7*(1), 62–73. http://doi.org/10.1016/j.chom.2009.12.002

Bushell, E., Gomes, A. R., Sanderson, T., Anar, B., Girling, G., Herd, C., et al. (2017). Functional profiling of a *Plasmodium* genome reveals an abundance of essential genes. *Cell*, *170*(2), 260–272. http://doi.org/10.1016/j.cell.2017.06.030

Crabb, B. S., & Cowman, A. F. (1996). Characterization of promoters and stable transfection by homologous and nonhomologous recombination in *Plasmodium falciparum*. *Proceedings of the National Academy of Sciences of the United States of America*, *93*(14), 7289–7294.

DeRocher, A. E., Karnataki, A., Vaney, P., & Parsons, M. (2012). Apicoplast targeting of a *Toxoplasma gondii* transmembrane protein requires a cytosolic tyrosine-based motif. *Traffic*, *13*(5), 694–704. http://doi.org/10.1111/j.1600-0854.2012.01335.x

Elsworth, B., Matthews, K., Nie, C. Q., Kalanon, M., Charnaud, S. C., Sanders, P. R., et al. (2014). PTEX is an essential nexus for protein export in malaria parasites.

*Nature*, *511*(7511), 587–591. http://doi.org/10.1038/nature13555

Fichera, M. E., Bhopale, M. K., & Roos, D. S. (1995). *In vitro* assays elucidate peculiar kinetics of clindamycin action against *Toxoplasma gondii*. *Antimicrobial Agents and Chemotherapy*, *39*(7), 1530–1537.

Fischer, K. (2011). The import and export business in plastids: transport processes across the inner envelope membrane. *Plant Physiology*, *155*(4), 1511–1519. http://doi.org/10.1104/pp.110.170241

Foth, B. J., Ralph, S. A., Tonkin, C. J., Struck, N. S., Fraunholz, M. J., Roos, D. S., et al. (2003). Dissecting apicoplast targeting in the malaria parasite *Plasmodium falciparum*. *Science*, *299*(5607), 705–708. http://doi.org/10.1126/science.1078599

Gisselberg, J. E., Dellibovi-Ragheb, T. A., Matthews, K. A., Bosch, G., & Prigge, S. T. (2013). The Suf iron-sulfur cluster synthesis pathway is required for apicoplast maintenance in malaria parasites. *PLOS Pathogens*, *9*(9), e1003655. http://doi.org/10.1371/journal.ppat.1003655.s009

Golldack, A., Henke, B., Bergmann, B., Wiechert, M., Erler, H., Blancke Soares, A., et al. (2017). Substrate-analogous inhibitors exert antimalarial action by targeting the *Plasmodium* lactate transporter *Pf*FNT at nanomolar scale. *PLOS Pathogens*, *13*(2), e1006172. http://doi.org/10.1371/journal.ppat.1006172

Gomes, A. R., Bushell, E., Schwach, F., Girling, G., Anar, B., Quail, M. A., et al. (2015). A genome-scale vector resource enables high-throughput reverse genetic screening in a malaria parasite. *Cell Host and Microbe*, *17*(3), 404–413. http://doi.org/10.1016/j.chom.2015.01.014

Goodman, C. D., Su, V., & McFadden, G. I. (2007). The effects of anti-bacterials on the malaria parasite *Plasmodium falciparum*. *Molecular and Biochemical Parasitology*, *152*(2), 181–191. http://doi.org/10.1016/j.molbiopara.2007.01.005

Hall, N., Karras, M., Raine, J. D., Carlton, J. M., Kooij, T. W. A., Berriman, M., et al. (2005). A comprehensive survey of the *Plasmodium* life cycle by genomic, transcriptomic, and proteomic analyses. *Science*, *307*(5706), 82–86. http://doi.org/10.1126/science.1103717

Hollingdale, M. R., Leland, P., & Schwartz, A. L. (1983). *In vitro* cultivation of the exoerythrocytic stage of *Plasmodium berghei* in a hepatoma cell line. *The American Journal of Tropical Medicine and Hygiene*, *32*(4), 682–684.

Janse, C. J., Ramesar, J., & Waters, A. P. (2006). High-efficiency transfection and drug selection of genetically transformed blood stages of the rodent malaria parasite *Plasmodium berghei*. *Nature Protocols*, *1*(1), 346–356. http://doi.org/10.1038/nprot.2006.53

Joët, T., & Krishna, S. (2004). The hexose transporter of *Plasmodium falciparum* is a worthy drug target. *Acta Tropica*, *89*(3), 371–374. http://doi.org/10.1016/j.actatropica.2003.11.003

Joët, T., Eckstein-Ludwig, U., Morin, C., & Krishna, S. (2003). Validation of the hexose transporter of *Plasmodium falciparum* as a novel drug target. *Proceedings of the National Academy of Sciences*, *100*(13), 7476–7479. http://doi.org/10.1073/pnas.1330865100

Kaur, J., & Bachhawat, A. K. (2009). A modified Western blot protocol for enhanced

sensitivity in the detection of a membrane protein. *Analytical Biochemistry*, *384*(2), 348–349. http://doi.org/10.1016/j.ab.2008.10.005

Ke, H., Sigala, P. A., Miura, K., Morrisey, J. M., Mather, M. W., Crowley, J. R., et al. (2014). The heme biosynthesis pathway is essential for *Plasmodium falciparum* development in mosquito stage but not in blood stages. *Journal of Biological Chemistry*, *289*(50), 34827–34837. http://doi.org/10.1074/jbc.M114.615831

Kenthirapalan, S., Waters, A. P., Matuschewski, K., & Kooij, T. W. A. (2016). Functional profiles of orphan membrane transporters in the life cycle of the malaria parasite. *Nature Communications*, *7*(10519). http://doi.org/10.1038/ncomms10519

Kirk, K. (2004). Channels and transporters as drug targets in the *Plasmodium*-infected erythrocyte. *Acta Tropica*, *89*(3), 285–298. http://doi.org/10.1016/j.actatropica.2003.10.002

Kirk, K., & Lehane, A. M. (2014). Membrane transport in the malaria parasite and its host erythrocyte. *Biochemical Journal*, *457*(1), 1–18. http://doi.org/10.1042/BJ20131007

Köhler, S., Delwiche, C. F., Denny, P. W., Tilney, L. G., Webster, P., Wilson, R. J., et al. (1997). A plastid of probable green algal origin in apicomplexan parasites. *Science*, *275*(5305), 1485–1489. http://doi.org/10.1126/science.275.5305.1485

Krishna, S., Webb, R., & Woodrow, C. (2001). Transport proteins of *Plasmodium falciparum*: defining the limits of metabolism. *International Journal for Parasitology*, *31*(12), 1331–1342.

Krishna, S., Woodrow, C. J., Burchmore, R. J., Saliba, K. J., & Kirk, K. (2000). Hexose transport in asexual stages of *Plasmodium falciparum* and kinetoplastidae. *Parasitology Today*, *16*(12), 516–521. http://doi.org/10.1016/S0169-4758(00)01762-2

Lehane, A. M., Ridgway, M. C., Baker, E., & Kirk, K. (2014). Diverse chemotypes disrupt ion homeostasis in the malaria parasite. *Molecular Microbiology*, *94*(2), 327–339. http://doi.org/10.1111/mmi.12765

Li, L., Stoeckert, C. J., Jr, & Roos, D. S. (2003). OrthoMCL: identification of ortholog groups for eukaryotic genomes. *Genome Research*, *13*(9), 2178–2189. http://doi.org/10.1101/gr.1224503

Lim, L., Linka, M., Mullin, K. A., Weber, A. P. M., & McFadden, G. I. (2010). The carbon and energy sources of the non-photosynthetic plastid in the malaria parasite. *FEBS Letters*, *584*(3), 549–554. http://doi.org/10.1016/j.febslet.2009.11.097

Lim, L., Sayers, C. P., Goodman, C. D., & McFadden, G. I. (2016). Targeting of a transporter to the outer apicoplast membrane in the human malaria parasite *Plasmodium falciparum*. *PLOS ONE*, *11*(7), e0159603. http://doi.org/10.1371/journal.pone.0159603.s002

Marchetti, R. V., Lehane, A. M., Shafik, S. H., Winterberg, M., Martin, R. E., & Kirk, K. (2015). A lactate and formate transporter in the intraerythrocytic malaria parasite, *Plasmodium falciparum*. *Nature Communications*, *6*(6721). http://doi.org/10.1038/ncomms7721

Martin, R. E., Ginsburg, H., & Kirk, K. (2009). Membrane transport proteins of the malaria parasite. *Molecular Microbiology*, *74*(3), 519–528. http://doi.org/10.1111/j.1365-2958.2009.06863.x

Martin, R. E., Henry, R. I., Abbey, J. L., Clements, J. D., & Kirk, K. (2005). The "permeome" of the malaria parasite: an overview of the membrane transport proteins of *Plasmodium falciparum*. *Genome Biology*, *6*(3), R26. http://doi.org/10.1186/gb-2005-6-3-r26

McFadden, G. I., & van Dooren, G. G. (2004). Evolution: red algal genome affirms a common origin of all plastids. *Current Biology*, *14*(13), R514–R516. http://doi.org/10.1016/j.cub.2004.06.041

McFadden, G. I., Reith, M. E., Munholland, J., & Lang-Unnasch, N. (1996). Plastid in human parasites. *Nature*, *381*(6582), 482. http://doi.org/10.1038/381482a0

McMillan, P. J., Millet, C., Batinovic, S., Maiorca, M., Hanssen, E., Kenny, S., et al. (2013). Spatial and temporal mapping of the *Pf*EMP1 export pathway in *Plasmodium falciparum*. *Cellular Microbiology*, *15*(8), 1401–1418. http://doi.org/10.1111/cmi.12125

Mullin, K. A., Lim, L., Ralph, S. A., Spurck, T. P., Handman, E., & McFadden, G. I. (2006). Membrane transporters in the relict plastid of malaria parasites. *Proceedings of the National Academy of Sciences*, *103*(25), 9572–9577. http://doi.org/10.1073/pnas.0602293103

Nagaraj, V. A., Sundaram, B., Varadarajan, N. M., Subramani, P. A., Kalappa, D. M., Ghosh, S. K., & Padmanaban, G. (2013). Malaria parasite-synthesized heme is

essential in the mosquito and liver stages and complements host heme in the blood stages of infection. *PLOS Pathogens*, *9*(8), e1003522. http://doi.org/10.1371/journal.ppat.1003522

Otto, T. D., Böhme, U., Jackson, A. P., Hunt, M., Franke-Fayard, B., Hoeijmakers, W. A. M., et al. (2014). A comprehensive evaluation of rodent malaria parasite genomes and gene expression. *BMC Biology*, *12*(86). http://doi.org/10.1186/s12915-014-0086-0

Pfander, C., Anar, B., Brochet, M., Rayner, J. C., & Billker, O. (2012). Recombination-mediated genetic engineering of *Plasmodium berghei* DNA. In *Malaria: methods and protocols* (Vol. 923, pp. 127–138). Totowa, NJ: New York, Humana, Springer distributor. http://doi.org/10.1007/978-1-62703-026-7_8

Pfander, C., Anar, B., Schwach, F., Otto, T. D., Brochet, M., Volkmann, K., et al. (2011). A scalable pipeline for highly effective genetic modification of a malaria parasite. *Nature Methods*, *8*(12), 1078–1082. http://doi.org/10.1038/nmeth.1742

Pick, T. R., & Weber, A. P. M. (2014). Unknown components of the plastidial permeome. *Frontiers in Plant Science*, *5*(410). http://doi.org/10.3389/fpls.2014.00410

Prommana, P., Uthaipibull, C., Wongsombat, C., Kamchonwongpaisan, S., Yuthavong, Y., Knuepfer, E., et al. (2013). Inducible knockdown of *Plasmodium gene* expression using the *glmS* ribozyme. *PLOS ONE*, *8*(8), e73783. http://doi.org/10.1371/journal.pone.0073783

Ralph, S. A., van Dooren, G. G., Waller, R. F., Crawford, M. J., Fraunholz, M. J.,

Foth, B. J., et al. (2004). Metabolic maps and functions of the *Plasmodium falciparum* apicoplast. *Nature Reviews Microbiology*, *2*(3), 203–216. http://doi.org/10.1038/nrmicro843

Rathnapala, U. L., Goodman, C. D., & McFadden, G. I. (2017). A novel genetic technique in *Plasmodium berghei* allows liver stage analysis of genes required for mosquito stage development and demonstrates that de novo heme synthesis is essential for liver stage development in the malaria parasite. *PLOS Pathogens*, *13*(6), e1006396. http://doi.org/10.1371/journal.ppat.1006396

Rijpma, S. R., van der Velden, M., Annoura, T., Matz, J. M., Kenthirapalan, S., Kooij, T. W. A., et al. (2016). Vital and dispensable roles of *Plasmodium* multidrug resistance transporters during blood- and mosquito-stage development. *Molecular Microbiology*, *101*(1), 78–91. http://doi.org/10.1111/mmi.13373

Rottmann, M., McNamara, C., Yeung, B. K. S., Lee, M. C. S., Zou, B., Russell, B., et al. (2010). Spiroindolones, a potent compound class for the treatment of malaria. *Science*, *329*(5996), 1175–1180. http://doi.org/10.1126/science.1193225

Saier, M. H. (2000). A functional-phylogenetic classification system for transmembrane solute transporters. *Microbiology and Molecular Biology Reviews*, *64*(2), 354–411.

Schindelin, J., Arganda-Carreras, I., Frise, E., Kaynig, V., Longair, M., Pietzsch, T., et al. (2012). Fiji: an open source platform for biological image analysis. *Nature Methods*, *9*(7), 676–682. http://doi.org/10.1038/nmeth.2019

Schmittgen, T. D., & Livak, K. J. (2008). Analyzing real-time PCR data by the

comparative $C_T$ method. *Nature Protocols*, *3*(6), 1101–1108. http://doi.org/10.1038/nprot.2008.73

Schwach, F., Bushell, E., Gomes, A. R., Anar, B., Girling, G., Herd, C., et al. (2015). *Plasmo*GEM, a database supporting a community resource for large-scale experimental genetics in malaria parasites. *Nucleic Acids Research*, *43*(Database issue), D1176–D1182. http://doi.org/10.1093/nar/gku1143

Sievers, F., Wilm, A., Dineen, D., Gibson, T. J., Karplus, K., Li, W., et al. (2011). Fast, scalable generation of high-quality protein multiple sequence alignments using Clustal Omega. *Molecular Systems Biology*, *7*(539). http://doi.org/10.1038/msb.2011.75

Smilkstein, M., Sriwilaijaroen, N., Kelly, J. X., Wilairat, P., & Riscoe, M. (2004). Simple and inexpensive fluorescence-based technique for high-throughput antimalarial drug screening. *Antimicrobial Agents and Chemotherapy*, *48*(5), 1803–1806.

Spillman, N. J., Allen, R. J. W., McNamara, C. W., Yeung, B. K. S., Winzeler, E. A., Diagana, T. T., & Kirk, K. (2013). $Na^+$ regulation in the malaria parasite *Plasmodium falciparum* involves the cation ATPase *Pf*ATP4 and is a target of the spiroindolone antimalarials. *Cell Host and Microbe*, *13*(2), 227–237. http://doi.org/10.1016/j.chom.2012.12.006

Trager, W., & Jensen, J. B. (1976). Human malaria parasites in continuous culture. *Science*, *193*(4254), 673–675. http://doi.org/10.1645/0022-3395(2005)091[0484:HMPICC]2.0.CO;2

Tusnády, G. E., & Simon, I. (1998). Principles governing amino acid composition of integral membrane proteins: application to topology prediction. *Journal of Molecular Biology*, *283*(2), 489–506. http://doi.org/10.1006/jmbi.1998.2107

Tusnády, G. E., & Simon, I. (2001). The HMMTOP transmembrane topology prediction server. *Bioinformatics*, *17*(9), 849–850.

van Dooren, G. G., & Striepen, B. (2013). The algal past and parasite present of the apicoplast. *The Annual Review of Microbiology*, *67*(1), 271–289. http://doi.org/10.1146/annurev-micro-092412-155741

van Schaijk, B. C. L., Kumar, T. R. S., Vos, M. W., Richman, A., van Gemert, G.-J., Li, T., et al. (2014). Type II fatty acid biosynthesis is essential for *Plasmodium falciparum* sporozoite development in the midgut of *Anopheles* mosquitoes. *Eukaryotic Cell*, *13*(5), 550–559. http://doi.org/10.1128/EC.00264-13

Weber, A. P. M., & Linka, N. (2011). Connecting the plastid: transporters of the plastid envelope and their role in linking plastidial with cytosolic metabolism. *Annual Review of Plant Biology*, *62*(1), 53–77. http://doi.org/10.1146/annurev-arplant-042110-103903

Weiner 3rd, J., & Kooij, T. W. A. (2016). Phylogenetic profiles of all membrane transport proteins of the malaria parasite highlight new drug targets. *Microbial Cell*, *3*(10), 511–521. http://doi.org/10.15698/mic2016.10.534

Woodrow, C. J., Penny, J. I., & Krishna, S. (1999). Intraerythrocytic *Plasmodium falciparum* expresses a high affinity facilitative hexose transporter. *Journal of Biological Chemistry*, *274*(11), 7272–7277.

http://doi.org/10.1074/jbc.274.11.7272

Wu, Y., Sifri, C. D., Lei, H.-H., Su, X.-Z., & Wellems, T. E. (1995). Transfection of *Plasmodium falciparum* within human red blood cells. *Proceedings of the National Academy of Sciences of the United States of America*, *92*(4), 973–977.

Yeh, E., & DeRisi, J. L. (2011). Chemical rescue of malaria parasites lacking an apicoplast defines organelle function in blood-stage *Plasmodium falciparum*. *PLOS Biology*, *9*(8), e1001138. http://doi.org/10.1371/journal.pbio.1001138.s009

Yu, M., Kumar, T. R., Nkrumah, L. J., Coppi, A., Retzlaff, S., Li, C. D., et al. (2008). The fatty acid biosynthesis enzyme FabI plays a key role in the development of liver-stage malarial parasites. *Cell Host and Microbe*, *4*(6), 567–578. http://doi.org/10.1016/j.chom.2008.11.001

Zhu, G., Marchewka, M. J., & Keithly, J. S. (2000). *Cryptosporidium parvum* appears to lack a plastid genome. *Microbiology*, *146*(Pt 2), 315–321. http://doi.org/10.1099/00221287-146-2-315

Zuegge, J., Ralph, S. A., Schmuker, M., McFadden, G. I., & Schneider, G. (2001). Deciphering apicoplast targeting signals - feature extraction from nuclear-encoded precursors of *Plasmodium falciparum* apicoplast proteins. *Gene*, *280*, 19–26.

## Table

**Table 1. Candidate apicoplast membrane proteins in *Plasmodium*.** Gene IDs are given for both *P. berghei* and *P. falciparum* orthologues and *Plasmo*DB annotations

are shown, distinguishing between putative membrane transporters and putative integral membrane proteins. If a gene name has been assigned, it is given in brackets after the annotation. Presence of a gene orthologue in *Toxoplasma gondii*, *Theileria*, *Babesia* and *Cryptosporidium* is indicated by '+' and absence is shown by '-'. [a]Transmembrane domains (TMD) were predicted in *P. falciparum* with TMHMM and TMpred. If there was a discrepancy, the TMHMM and strongest TMpred results are given (TMHMM/TMpred). [b]Localisation was predicted with *Plasmo*AP and PATS in *P. falciparum*. [c]*P. berghei* normalised expression for rings (R), trophozoites (T), schizonts (S) and gametocytes (G) (Otto et al., 2014), was binned with thresholds on sample percentiles: 0-5% (Very low), 5-25% (Low), 25-75% (Moderate), 75-95% (High), 95-100% (Very high). For results: ND = no data, *localised in *P. falciparum*, [α]Rijpma et al. (2016), [β]contradicted by Kenthirapalan et al. (2016), [θ]confirmed by Rijpma et al. (2016), [γ]Kenthirapalan et al. (2016), [δ]confirmed by Kenthirapalan et al. (2016), [§]contradicted by Rijpma et al. (2016), [ν]confirmed by Bushell et al. (2017), [λ]contradicted by Bushell et al. (2017), [Ω]mutant displays significantly slow growth (Bushell et al., 2017). Each candidate was categorised by colour depending on blood stage essentiality and localisation results displayed in Figure 4.

## Figures

**Figure 1. Candidate gene knockout PCR screen and reverse transcriptase-PCR in *P. berghei*.** A: PCR was performed on wild-type (WT) *Pb*ANKA and candidate gene knockout (KO) genomic DNA (gDNA) extracted from mixed population blood

stage parasites. WT locus and integrant primers were used. PCR product bands were cropped from the correct well at the predicted product size of an ethidium bromide-stained agarose gel image. The *Pb*ANKA_1364800 KO integrant primers span the entire KO construct with less than a 650 bp size difference between the WT and KO predicted products, so both the WT and KO products are observed in the cropped region of the agarose gel indicating that both the WT locus and integrated KO vector are present in the parasite population. B: Three primer pairs were designed within the *Pb*ANKA_0401200 coding sequence (CDS) to detect RNA expression, primers 1 (red), 2 (green) and 3 (blue). Primer positions and fragment sizes are shown on the gene schematic. RNA was extracted from clonal *Pb*ANKA_0401200 KO parasites and reverse-transcribed into cDNA. C: Tubulin primers were included and each primer pair was used to amplify WT *Pb*ANKA gDNA (positive controls) and *Pb*ANKA_0401200 KO cDNA. No template control (NTC) and PCR reactions without reverse transcriptase (no RT) were used as negative controls. Reactions were electrophoresed and PCR product bands were cropped from the correct well at the predicted product size of an ethidium bromide-stained agarose gel image. Primer type is given on left and sample type is given above.

**Figure 2. Tagged candidate protein expression and *Pf*3D7_0716900-*glmS* knockdown.** A: Western blot analysis was performed on each HA-tagged (TAG) candidate in *P. berghei*. Parasite protein was extracted and separated by SDS-PAGE, transferred to a membrane, and visualised by probing with rat anti-HA primary and

anti-rat HRP secondary antibodies. Protein band masses are shown by a standard marker (left). Parasite protein was extracted during the blood stage, except for *Pb*ANKA_0809500 TAG, which was taken from sporozoites. B: *Pf*3D7_1145500-GFP (ABCB3) blood stage expression. Protein was probed with mouse anti-GFP primary and anti-mouse HRP secondary antibodies. Western blots were also performed once on protein extracted from the following sorbitol-synchronised parasites over 120 hours: (C) *Pf*3D7_0716900-*glmS* (DMT2-*glmS* clone B11) without glucosamine (GlcN) and (D) DMT2-*glmS* clone B11 with GlcN. Molecular mass markers are shown on left and antibodies are given on right. Anti-HA was used to monitor DMT2-*glmS* expression and anti-BiP as a protein loading control. Wild-type (WT) 3D7 protein was included as a negative control for non-specific antibody binding. To quantify protein expression, the data were normalised to BiP by calculating the ratio of HA to BiP signal (E) to compare DMT2-*glmS* expression with and without GlcN.

**Figure 3. Immunolocalisation of putative membrane proteins in *Plasmodium*.** A: *P. berghei* and *P. falciparum* (*Pf*DMT2-*glmS* clone D6, *Pf*ABCB4-HA clone G3, *Pf*ABCB4-*glmS* clone F11) candidate proteins were HA-tagged and probed with rat anti-HA primary and anti-rat 488 secondary antibodies (green). The apicoplast was probed with rabbit anti-ACP primary and anti-rabbit 546 secondary antibodies (red) and nuclei were stained with Hoechst (blue). Channels were merged with a transmission image (right) showing the location within the parasite. All candidates

were localised within red blood cell stage parasites except *Pb*ANKA_0809500, which was localised in a sporozoite. Scale bars are 2 µm. B: *Pf*3D7_1145500-GFP was localised in an intraerythrocytic parasite probed with mouse anti-GFP primary and anti-mouse 488 secondary antibodies (green; scale bar is 2 µm). C: *Pb*ANKA_1103600 TAG parasites were localised in oocyst, sporozoite and *in vitro* liver cell stage parasites. Scale bars are 5 µm. D: Seven candidates were also localised to non-apicoplast structures within intraerythrocytic parasites (scale bars are 2 µm).

**Figure 4. Screening results for candidate apicoplast membrane proteins in *Plasmodium*.** Blood stage essentiality (Essential or Non-essential) and localisation (Apicoplast or Non-apicoplast) data was collected for 27 candidates. As shown in Table 1, each candidate was placed into one of the following categories: Essential, Apicoplast/Essential, Apicoplast, Apicoplast/Non-essential, Non-essential, Non-apicoplast/Non-essential, Non-apicoplast or Non-apicoplast/Essential. Proteins for which gene deletion or localisation data were not available are presented in a single category (Essential, Apicoplast, Non-essential or Non-apicoplast).

**Figure 5. Candidate gene PCR screen in *P. falciparum*.** PCR was performed on wild-type (WT) 3D7, *Pf*3D7_0302600-HA (clone G3) and *Pf*3D7_0716900-*glmS* (clone B11) genomic DNA (gDNA) extracted from blood stage parasites. WT locus and integrant primers were used. PCR product bands were cropped from the correct well at the predicted product size of an ethidium bromide-stained agarose gel image.

**Figure 6. *Pf*3D7_0716900 knockdown IPP supplementation growth assay and parasite morphology.** In one replicate, sorbitol-synchronised *Pf*3D7_0716900-*glmS* (DMT2-*glmS* clone B11) and *Pf*3D7_0302600-HA (ABCB4-HA clone G3) control parasites were grown for up to 12 days with or without IPP and glucosamine (GlcN). A: Treatment timelines for each culture are shown in the colour-coded table. As controls, HA parasites were grown with IPP and GlcN (+IPP+GlcN), and *glmS* parasites were grown without IPP and GlcN (-IPP-GlcN) for six days. On day six, cultures were discontinued, continued with the same treatment or continued with a different treatment. Colour links a continued culture with the original culture (cultures coloured light blue, purple and green, all originate from the same +IPP+GlcN culture coloured dark blue). Growth was monitored by daily blood smears and parasitaemia was determined by calculating the percentage of infected red blood cells. Parasite growth is shown in B. Dotted vertical lines on the graph every two days indicate when the cultures were subbed. 'x' indicates when a culture was discontinued. C: Parasite morphology was monitored by daily blood smears.

**Figure 7. Organellar DNA in *Pf*3D7_0716900 knockdown IPP rescued parasites.** The ratio of mitochondrion and apicoplast DNA to nuclear DNA in IPP rescued parasites relative to wild-type (WT) parasites was measured by real-time PCR. Genomic DNA was extracted from WT 3D7 parasites, *Pf*3D7_0716900-*glmS* (DMT2-*glmS* clone B11) parasites growing without treatment (-IPP-GlcN) and with IPP and

glucosamine (GlcN) for 12 days (+IPP+GlcN). *Pf*3D7_0302600-HA (ABCB4-HA clone G3) parasites growing without treatment (-IPP-GlcN) were included as a positive control. Reactions were performed in triplicate and the organellar to nuclear DNA (1.0) ratio was normalised relative to WT levels.

**Figure 8. Novel apicoplast putative membrane proteins in *Plasmodium*.** The two previously characterised apicoplast membrane transporters, iTPT and oTPT, are shown on the inner and outer membranes. Dependent on whether they have an apicoplast leader, the predicted positions of five novel apicoplast putative membrane transporters (orange), and two novel apicoplast putative integral membrane proteins (blue), are shown. Membrane proteins with a leader are predicted to localise to the inner apicoplast membrane, as iTPT does. Candidates without a leader are predicted to localise to the outer apicoplast membrane, as oTPT does.

## Supplementary tables

**Supplementary table 1. *Plasmo*GEM transfection vector identification numbers.** Listed are all *P. berghei* candidate genes with *Plasmo*GEM knockout (KO) and HA-tag (TAG) transfection vectors and their corresponding *Plasmo*GEM ID numbers.

**Supplementary table 2. Knockout construct cloning primers.** Listed are the 5' and 3' homologous gene specific flank primer sequences for the three knockout (KO) constructs made. Cloning restriction enzyme sites are in bold. *Pb*ANKA_0942100 KO

and *Pb*ANKA_0401200 KO 5' flanks include EcoRI and XhoI sites, and the 3' flanks include SacII and HindIII sites. The *Pb*ANKA_0505500 KO 5' flank includes SacII and BglII sites, and the 3' flank includes XhoI and NotI sites. Product sizes are given for each primer pair.

**Supplementary table 3. *P. falciparum* knockdown construct cloning primers.** Listed are the primer pairs designed for each *P. falciparum* construct made. One 3' homologous flank was made for each single crossover ribozyme construct. Cloning restriction enzyme sites added to each primer are in bold. Both ribozyme constructs use BglII and PstI. The product sizes for each primer pair are also shown.

**Supplementary table 4. Candidate gene knockout PCR screening primers.** Genomic DNA was extracted from wild-type (WT) *Pb*ANKA parasites and parasites from each candidate gene knockout (KO) transfection and screened with WT locus, integrant and KO vector primers. Whilst most integrant PCR primers only span the region at which one vector homologous flank meets the genome, three integrant primers span the entire KO vector[#^~]. In these cases, the integrated KO vector product size is given and presence of the WT locus gives a product of [#]1931 bp, [^]3057 bp and [~]2567 bp.

**Supplementary table 5. Candidate gene HA-tag PCR screening primers.** Parasites from each candidate gene HA-tag (TAG) transfection were screened with wild-type (WT) locus and TAG vector primers. Product sizes are listed for each primer pair.

**Supplementary table 6. *Pf*3D7_0302600 and *Pf*3D7_0716900 ribozyme construct PCR screening primers.** Parasite genomic DNA was extracted from *glmS* and HA transfected *P. falciparum* parasites and screened with wild-type (WT) locus and integrant primers. Restriction enzyme sites (SacII) are shown in bold in the reused *Pf*3D7_0716900 KO 5' flank cloning primers. Product sizes are given for each primer pair.

**Supplementary table 7. Reverse transcriptase-PCR primers.** Three primer pairs were designed within the wild-type (WT) *Pb*ANKA_0401200 coding sequence to determine whether the gene is being expressed in knockout parasites. Tubulin primers were used as a positive control. Product sizes are given for each primer pair.

**Supplementary table 8. Real-time PCR primer pairs.** For relative quantification, primers were designed to target genes in the mitochondrial, apicoplast and nuclear genomes. Cytochrome B (CytB) was targeted in the mitochondria, elongation factor Tu (TufA) was targeted in the apicoplast and beta-tubulin (β-Tubulin) was targeted in the nucleus. Product sizes are given for each primer pair.

## Supplementary figures

**Supplementary figure 1. Candidate gene knockout PCR screen in *P. berghei*.**

PCR was performed on wild-type (WT) *Pb*ANKA and candidate gene knockout (KO) genomic DNA (gDNA) extracted from mixed population blood stage parasites. WT locus, integrant and KO vector primers were used. KO vector primers were used for an initial screen for the presence of the KO vector before confirming presence of the integrated KO vector with the integrant primers, which typically had large PCR products. KO vector PCRs were not performed for three candidates (N/A) as their homologous flanks were small and therefore integration PCRs were not technically challenging. PCR product bands were cropped from the correct well at the predicted product size of an ethidium bromide-stained agarose gel image. The *Pb*ANKA_1364800 KO integrant primers span the entire KO construct with less than a 650 bp size difference between the WT and KO predicted products, so both the WT and KO products are observed in the cropped region of the agarose gel indicating that both the WT locus and integrated KO vector are present in the parasite population.

**Supplementary figure 2. *Pb*ANKA_0614600 knockout Southern blot analysis.**

Two restriction enzyme digestions were used to cut wild-type (WT) *Pb*ANKA and *Pb*ANKA_0614600 knockout (KO) genomic DNA (gDNA), PacI and HindIII. A: PacI cuts WT gDNA to produce a 5.4 kb fragment and produces a 9.1 kb fragment from *Pb*ANKA_0614600 KO gDNA. B: HindIII cuts WT gDNA around the *Pb*ANKA_0614600 coding sequence producing a 3.2 kb fragment. This digest

produces a 6.0 kb fragment when the KO construct has been successfully integrated. C: Digested gDNA was electrophoresed, transferred and fixed to a membrane that was then hybridised with the *Pb*ANKA_0614600 5' flank (2000 second exposure) and DHFR (4000 second exposure) probes. Fragment sizes are shown on left and sample type is noted above each lane.

**Supplementary figure 3. *Pb*ANKA_0942100 knockout Southern blot analysis.** Two restriction enzyme digestion combinations were used to cut wild-type (WT) *Pb*ANKA and *Pb*ANKA_0942100 knockout (KO) genomic DNA (gDNA), BamHI/SphI and EcoRI/SpeI. A: BamHI/SphI cuts around the coding sequence three times, producing 8.8 kb and 0.5 kb fragments. The KO construct introduces two new sites, producing 4.1 kb, 1.3 kb, 3.8 kb and 0.5 kb sized fragments. B: EcoRI and SpeI cut WT gDNA four times around the *Pb*ANKA_0942100 coding sequence, producing DNA fragments of 2.6 kb, 2.2 kb and 0.6 kb in size. This enzyme combination produces different fragments from *Pb*ANKA_0942100 KO gDNA that are 4.4 kb, 0.8 kb and 0.6 kb in size. C: Digested gDNA was electrophoresed on an agarose gel and transferred to a membrane and fixed. Fixed gDNA was hybridised with *Pb*ANKA_0942100 5' flank (400 second exposure) and DHFR (800 second exposure) probes. Fragment sizes are given on left and sample type is marked above each lane.

**Supplementary figure 4. Spanning PCR on *Pb*ANKA_0942100 knockout parasites.** *Pb*ANKA_0942100 5' flank forward and 3' flank reverse primers were

used to amplify the gene. The wild-type (WT) locus produces a product of 3.7 kb compared to successful homologous recombination of the *Pb*ANKA_0942100 knockout (KO) construct which produces a PCR product of 4.1 kb. PCR reactions were performed on WT *Pb*ANKA and *Pb*ANKA_0942100 KO (replicate 3) genomic DNA (gDNA) and electrophoresed on an ethidium bromide-stained agarose gel. Both WT and KO gDNA produce product bands of 3.7 kb, the expected size resulting from the WT locus. Product sizes are given on left.

**Supplementary figure 5. Clonal *Pb*ANKA_0401200 knockout PCR screen.** PCR was performed on wild-type (WT) *Pb*ANKA and clonal candidate gene knockout (KO) genomic DNA (gDNA). PCR products were electrophoresed on an ethidium bromide-stained agarose gel. *Pb*ANKA_0401200 KO WT locus and integrant primers were used.

**Supplementary figure 6. *Pb*ANKA_0401200 knockout Southern blot analysis.** Two restriction enzyme digestions were used to cut wild-type (WT) and knockout (KO) genomic DNA, PacI and HpaI. A: PacI cuts WT gDNA on either side of the *Pb*ANKA_0401200 coding region producing a 5.7 kb fragment. Homologous recombination deleting the coding region shortens this fragment to 4.3 kb. B: HpaI cuts WT gDNA 5' to the coding region and twice within the 3' flank of *Pb*ANKA_0401200 coding region. Homologous recombination of the KO construct introduces another HpaI site, producing different fragment sizes for WT and KO

gDNA (6.3 kb and 4.8 kb). The size differences between WT and KO gDNA can be observed when probing with the *Pb*ANKA_0401200 5' flank probe. The DHFR probe detects presence of the DHFR sequence in parasite gDNA. C: Digested WT and KO gDNA fixed to a membrane was probed with the 5' flank (733 second exposure) and DHFR (3222 second exposure) probes. Fragment sizes are given on left and gDNA and digest type are marked above each lane.

**Supplementary figure 7. Candidate gene HA-tag PCR screen in *P. berghei*.** PCR was performed on wild-type (WT) *Pb*ANKA and candidate gene HA-tag (TAG) genomic DNA (gDNA) extracted from a mixed population of blood stage parasites. WT locus and TAG vector primers were used. PCR product bands were cropped from the correct well at the predicted product size of an ethidium bromide-stained agarose gel image.

**Supplementary figure 8. Ribozyme and control construct HA-tag protein expression in *P. falciparum*.** Western blots were performed on (A) *Pf*3D7_0302600-HA control (HA clone G3 and HA clone F8), *Pf*3D7_0302600-*glmS* (*glmS* clone G10 and *glmS* clone F11), and (B) *Pf*3D7_0716900-*glmS* (clones D6 and B11) parasites. Parasite protein was extracted and separated by SDS-PAGE, transferred to a membrane and visualised by probing with anti-HA primary and anti-rat HRP secondary antibodies. Protein band masses are shown with a standard marker (left).

**Supplementary figure 9. Ribozyme and control construct PCR screen in *P. falciparum*.** PCR was performed on wild-type (WT) 3D7 genomic DNA (gDNA) and each *Pf*3D7_0302600-HA, *Pf*3D7_0302600-*glmS* and *Pf*3D7_0716900-*glmS* clone transfectant gDNA extracted from cultured blood stage parasites. WT locus and integrant primers were used. PCR product bands were cropped from the correct well at the predicted product size of an ethidium bromide-stained agarose gel image.

**Supplementary figure 10. Wild-type 3D7, *Pf*3D7_0302600-HA and *Pf*3D7_0302600-*glmS* parasite growth with glucosamine.** Sorbitol-synchronised wild-type 3D7 (WT 3D7), *Pf*3D7_0302600-HA (ABCB4-HA) clone F8 and G3, and *Pf*3D7_0302600-*glmS* (ABCB4-*glmS*) clone F11 and G10 parasites were grown in triplicate with 0 mM to 10 mM glucosamine (GlcN) for 72 hours. Parasite growth was measured in a SYBR Green assay and normalised parasitaemia was calculated in comparison to no drug and no parasite controls. Log transformation of data was performed and standard deviation bars are shown.

**Supplementary figure 11. *Pf*3D7_0716900-*glmS* expression with and without glucosamine.** Western blots were performed once on protein extracted from the following sorbitol-synchronised parasites over 120 hours: (A) *Pf*3D7_0716900-*glmS* (DMT2-*glmS*) clone B11 without glucosamine (GlcN), (B) DMT2-*glmS* clone B11 with GlcN and (C) DMT-*glmS* clone D6 with GlcN. Molecular mass markers are shown on left and antibodies are given on right. Anti-HA was used to monitor DMT2-

*glmS* expression and anti-BiP as a protein loading control. Wild-type (WT) 3D7 protein was included as a negative control for non-specific antibody binding. To quantify protein expression, the data were normalised to BiP by calculating the ratio of HA to BiP signal (D) to compare DMT2-*glmS* clone B11 expression without GlcN (-GlcN) to DMT-*glmS* clone B11 and D6 expression with GlcN (+GlcN).

**Supplementary figure 12. *Pf*3D7_0302600 expression with glucosamine.** Western blots were performed once on protein extracted from sorbitol-synchronised (A) *Pf*3D7_0302600-HA (clone F8) and (B) *Pf*3D7_0302600-*glmS* (clone G10) parasites growing with 2.5 mM glucosamine (GlcN) over a 120-hour period. Molecular mass markers are shown on left and antibodies are given on right. Anti-HA was used to monitor *Pf*3D7_0302600 expression and anti-BiP as a protein loading control. Wild-type (WT) 3D7 protein was included as a negative control for non-specific antibody binding. To quantify protein expression, the data were normalised to BiP by calculating the ratio of HA to BiP signal (C) to compare *Pf*3D7_0302600-HA to *Pf*3D7_0302600-*glmS* expression in response to GlcN.

**Supplementary figure 13. *Pf*3D7_0716900-*glmS* clone D6 IPP supplementation growth assay and protein expression.** In one replicate, sorbitol-synchronised *Pf*3D7_0716900-*glmS* (DMT2-*glmS* clone D6) and *Pf*3D7_0302600-HA (ABCB4-HA clone F8) control parasites were grown for up to 18 days with or without IPP and glucosamine (GlcN). A: Treatment timelines for each culture are shown in the colour-

coded table. As controls, HA parasites were grown with IPP and GlcN (+IPP+GlcN) and *glmS* parasites were grown without treatment (-IPP-GlcN) for 12 days. On day 12, cultures were discontinued, continued with the same treatment or continued with a different treatment. Colour links a continued culture with the original culture (the four cultures coloured light blue, purple, green and yellow-green, all originated from the same +IPP+GlcN culture coloured dark blue). *IPP was removed from culture on day 14. 'x' indicates when a culture was discontinued. Growth was monitored by daily blood smears and parasitaemia was determined by calculating the percentage of infected red blood cells. Parasite growth is shown in B. Vertical dotted lines on the graph every two days indicate when the cultures were subbed. Parasite protein was extracted from (C) ABCB4-HA, (D) wild-type (WT) 3D7 (no treatment) and DMT2-*glmS* parasites throughout the growth assay. ABCB4-HA parasites with no treatment (-IPP-GlcN) were harvested from a culture being maintained. Protein was probed with anti-BiP, anti-HA and anti-ACP primary antibodies and anti-rat and anti-rabbit HRP secondary antibodies, for a protein loading control (BiP), to visualise expression of the HA-tagged protein and to determine presence of the apicoplast on the basis of expression of an apicoplast protein (ACP). WT protein was included as a negative control for non-specific antibody binding.

**Supplementary figure 14. Organellar DNA in *Pf*3D7_0716900 knockdown IPP rescued parasites.** The ratio of mitochondrion and apicoplast DNA to nuclear DNA in IPP rescued parasites relative to wild-type (WT) parasites was measured by real-

time PCR. Genomic DNA was extracted from WT 3D7 parasites, *Pf*3D7_0716900-*glmS* (DMT2-*glmS* clone D6) parasites growing without treatment (-IPP-GlcN), with only IPP (+IPP-GlcN) for 12 days and with IPP and GlcN (+IPP+GlcN) and 12 days and 18 days (*). Genomic DNA was also extracted for *Pf*3D7_0302600-HA (ABCB4-HA clone F8) control parasites growing without treatment (-IPP-GlcN) and with IPP and GlcN (+IPP+GlcN) for 12 days. Reactions were performed in triplicate and the organellar to nuclear DNA (1.0) ratio was normalised relative to WT levels.

**Supplementary figure 15. Apicoplast loss in IPP rescued *Pf*3D7_0716900 knockdown parasites.** HA-tagged, *Pf*3D7_0716900-*glmS* (clone D6) parasites were grown without IPP and glucosamine (GlcN) (-IPP-GlcN) and with IPP and GlcN (+IPP+GlcN) for 18 days. Red blood cell stage parasites were fixed and probed with anti-HA primary and anti-rat 488 secondary antibodies (green). For co-localisation, the apicoplast was probed with anti-ACP primary and anti-rabbit 546 secondary antibodies (red). Nuclei were stained with Hoechst (blue). Channels were merged with a transmission image (right) showing the location within the parasite. Scale bars are 2 μm.

**Supplementary figure 16. Tyrosine conservation in leaderless apicoplast putative membrane transporters.** Protein alignments were performed for orthologues of each leaderless apicoplast-localised candidate gene, *Pb*ANKA_0614600, *Pb*ANKA_1103600 and *Pb*ANKA_1304700. *Pb*ANKA_1107900 (oTPT) was

included as a positive control. Gene identification numbers for each orthologue are given on left and the first amino acid in each protein follows a '1'. The first transmembrane domain is bold and each tyrosine (Y) is highlighted a shade of red, depending of the level of conservation (i.e. 1 Y at a position in all orthologues is highlighted the lightest shade of red and 5 or more Y at a position in the orthologues are highlighted the darkest shade of red, indicating high conservation).

**Supplementary figure 17. Double crossover homologous recombination transfection strategy.** The linear transfection vector finds regions of the *P. berghei* genome homologous to the 5' and 3' flanks and replaces the candidate gene coding region to (A) knockout (KO) or (B) HA-tag (TAG) the gene, also introducing the DHFR selectable marker. Arrows represent typical forward and reverse PCR screening primer locations designed to identify the WT locus (green), integrant (red) and presence of the KO or TAG vector (blue). A: The KO strategy can result in successful homologous integration (gene disrupted) or random integration (gene not disrupted). B: TAG PCR screening primers identify the presence of the transfection vector. Schematic not to scale.

**Supplementary figure 18. Ribozyme knockdown strategy in *P. falciparum.*** A: The *glmS* ribozyme plasmid contains a 3' homologous flank, HA-tag, *glmS* ribozyme element and DHFR selectable marker. Homologous integration occurs at the 3' end of the candidate gene coding region causing the gene of interest to be HA-tagged and

regulated by addition of glucosamine which binds and activates the *glmS* ribozyme. B: The HA plasmid serves as a ribozyme control construct, to control for the effects of integration, and results in the gene of interest being HA-tagged. Both parasite lines can be positively selected by DHFR. Two primer pairs were designed to genotype the transfected parasites and their locations are indicated with arrows. WT locus primers are green and integrant primers are red.

**Supplementary figure 19. DHFR probe sequence.**

**Supplementary figure 20. Real-time PCR primer pair standard curves.** The mitochondrion primer pair has a standard curve with an $R^2$ value of 0.997 (A), the apicoplast primer pair has a standard curve with an $R^2$ value of 0.996 (B) and the nucleus primer pair has a standard curve with an $R^2$ value of 0.994 (C).

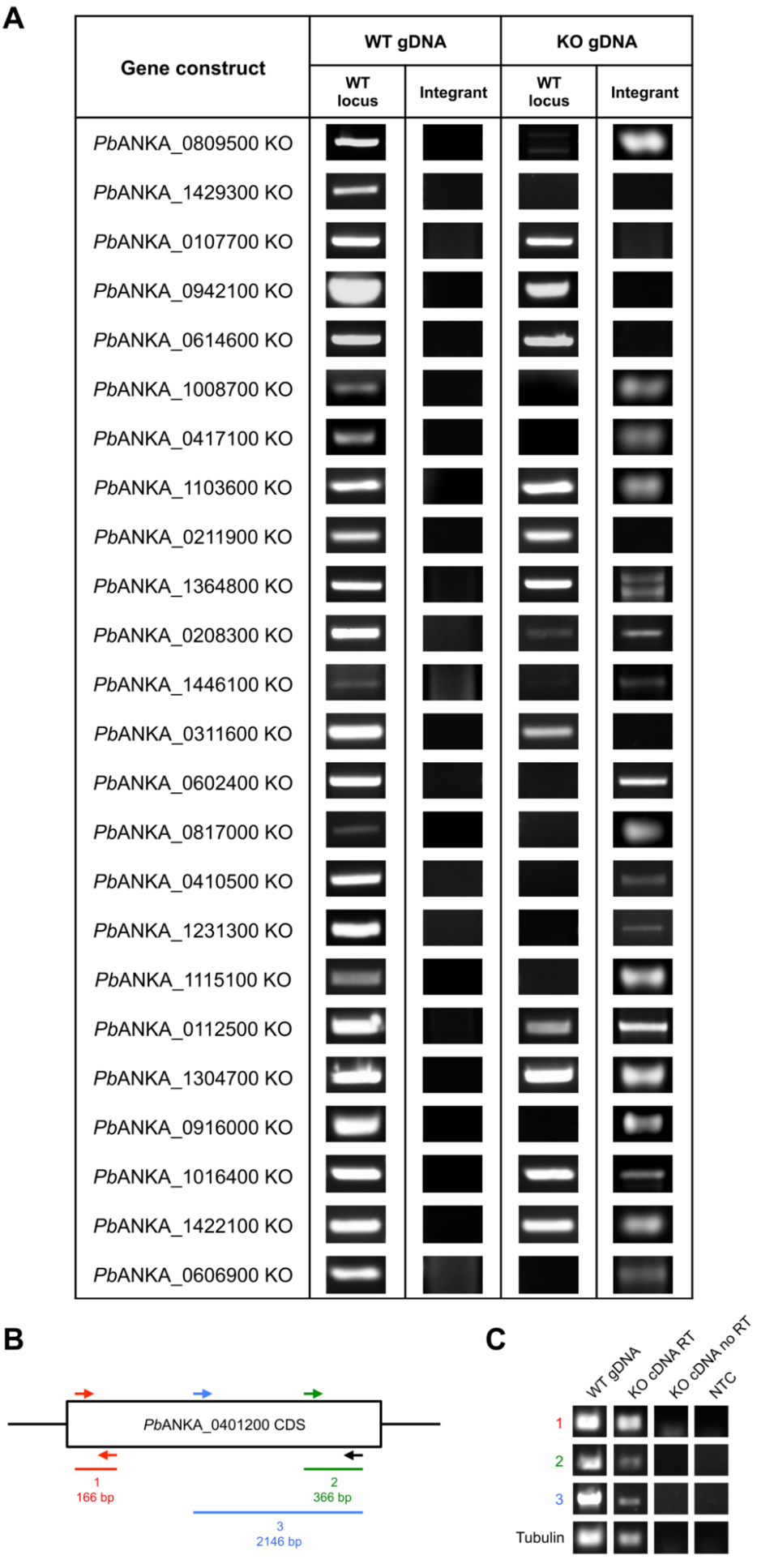


CMI_12789_F1.tiff

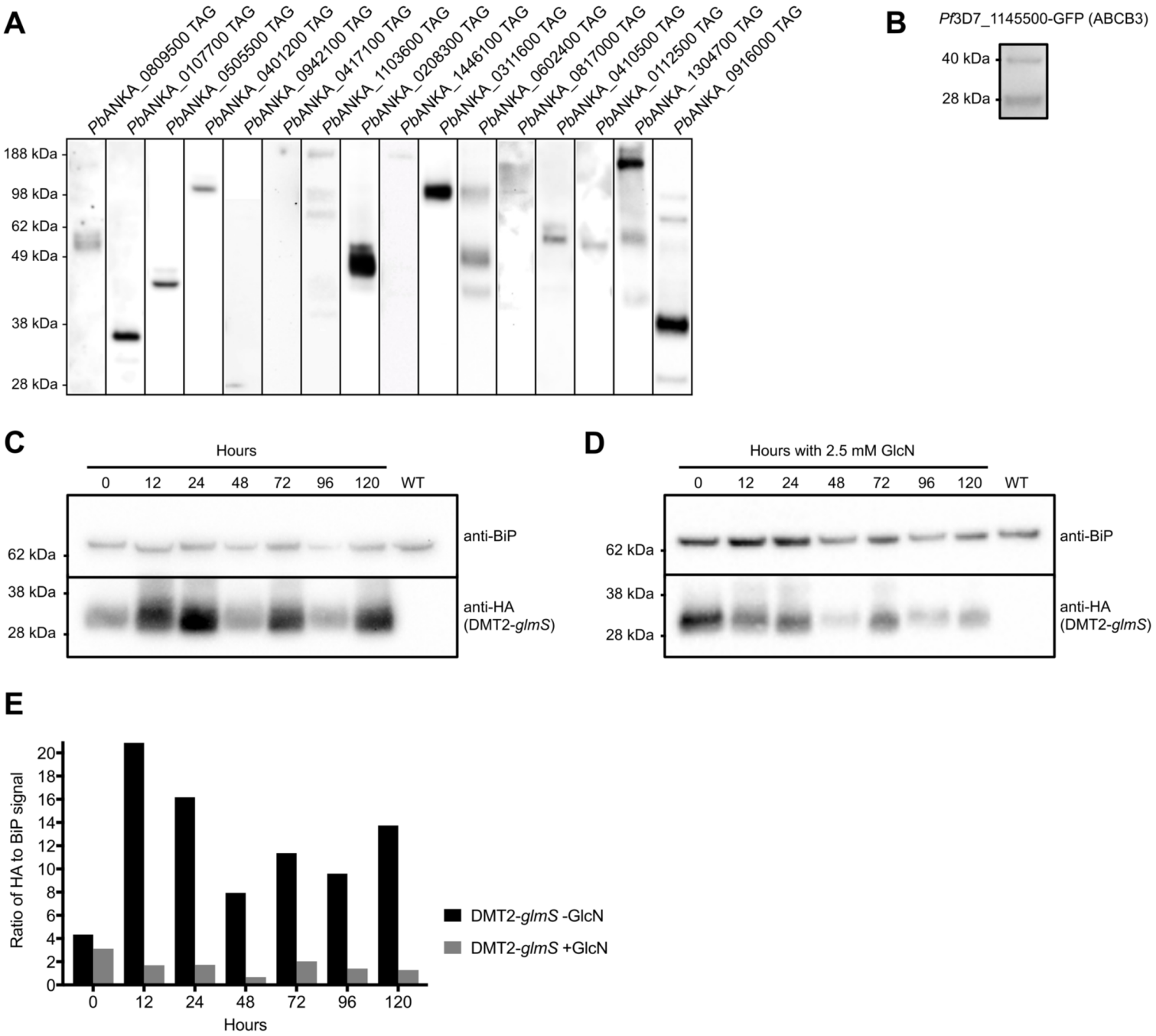


CMI_12789_F2.tiff

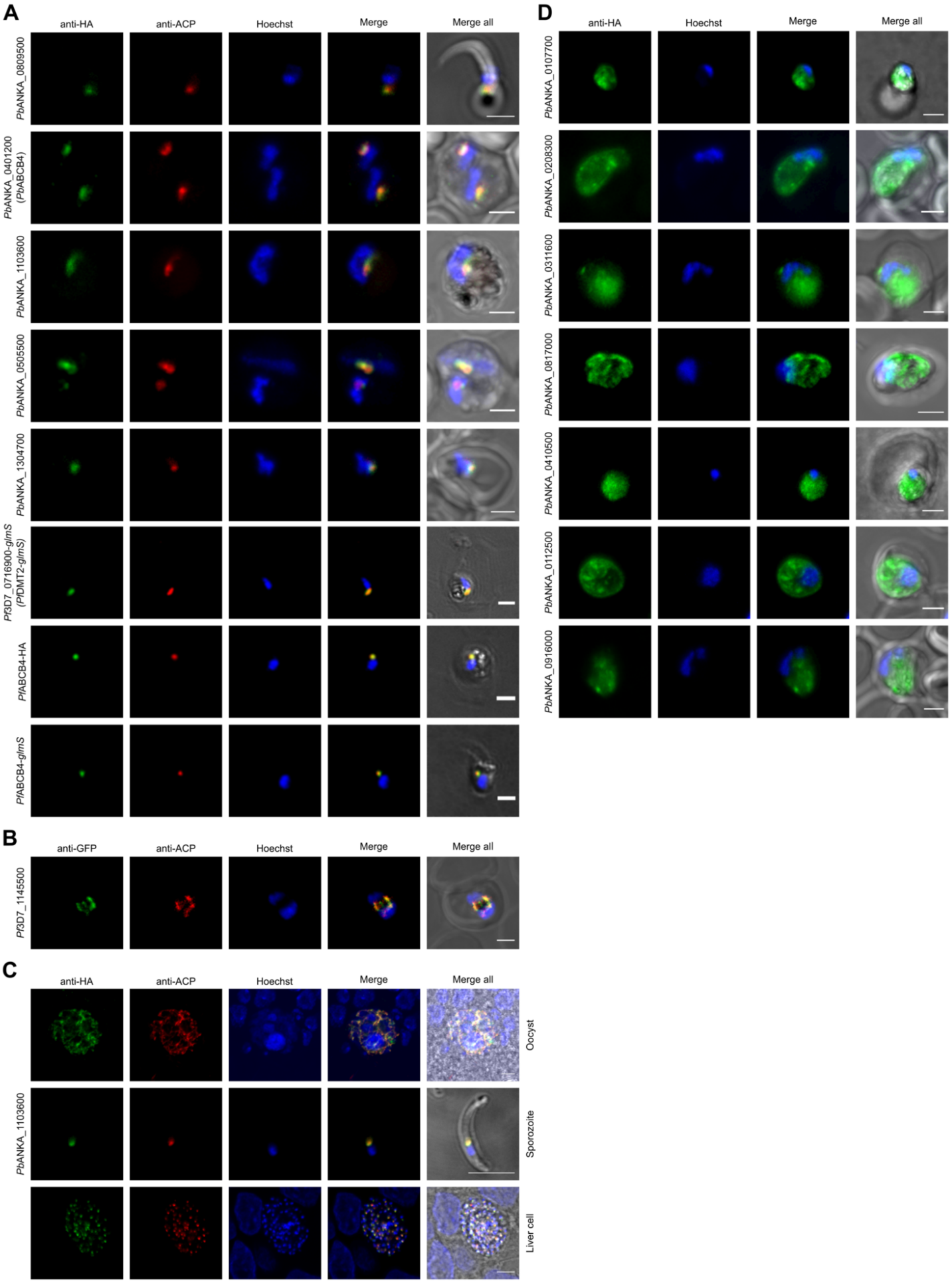


CMI_12789_F3.tiff

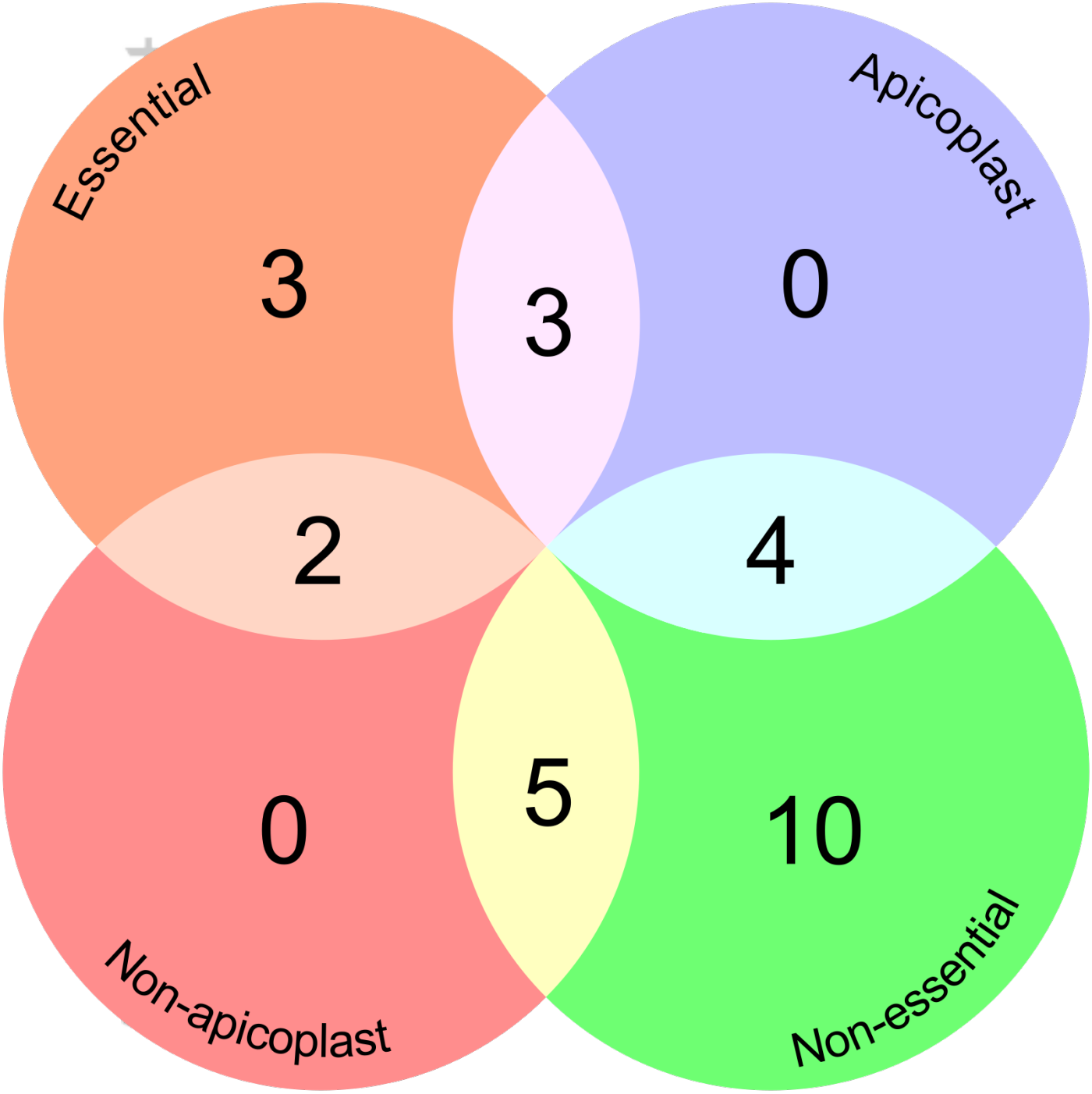


CMI_12789_F4.tiff

| Gene construct | WT gDNA | | Transfectant gDNA | |
|---|---|---|---|---|
| | WT locus | Integrant | WT locus | Integrant |
| *Pf*3D7_0302600-HA | 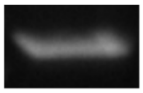 |  |  | 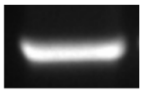 |
| *Pf*3D7_0716900-*glmS* | 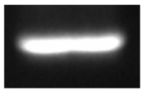 |  |  | 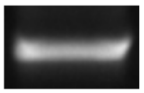 |

CMI_12789_F5.tiff

A

| Parasite line | Treatment | | | |
|---|---|---|---|---|
| | Day 0 - 6 | | Day 6 - 12 | |
| | IPP | GlcN | IPP | GlcN |
| *Pf*3D7_0302600-HA (ABCB4-HA) | + | + | × | |
| *Pf*3D7_0716900-*glmS* (DMT2-*glmS*) | - | - | × | |
| | - | + | × | |
| | + | - | - | - |
| | + | + | + | + |
| | | | + | - |
| | | | - | + |
| | | | - | - |

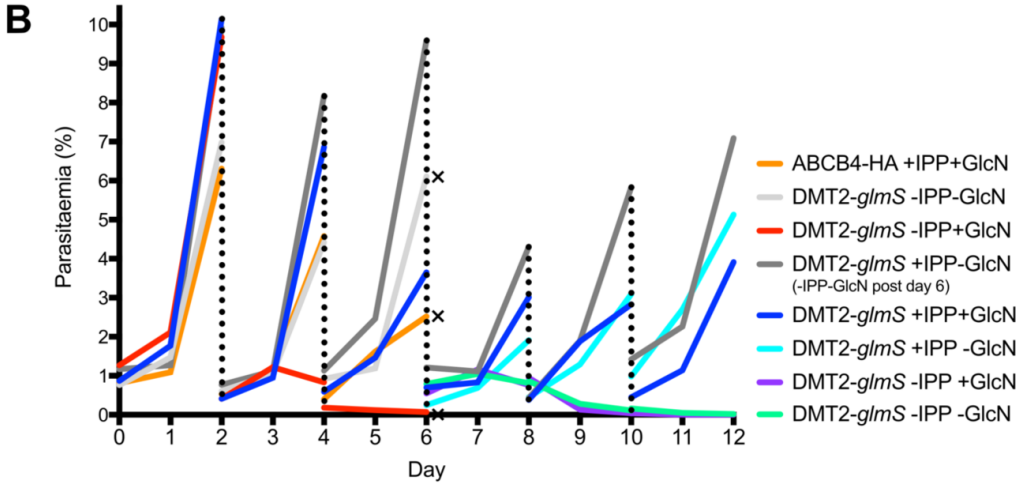


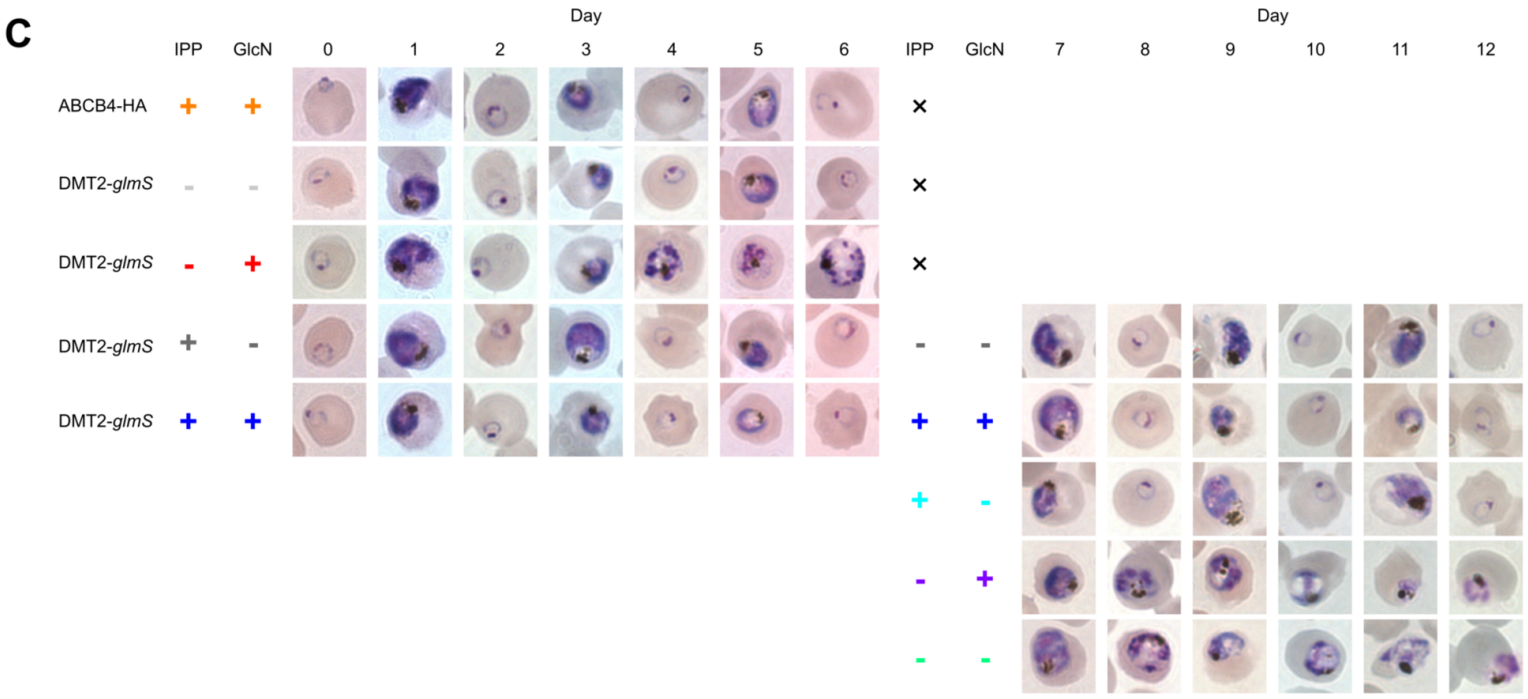


CMI_12789_F6.tiff

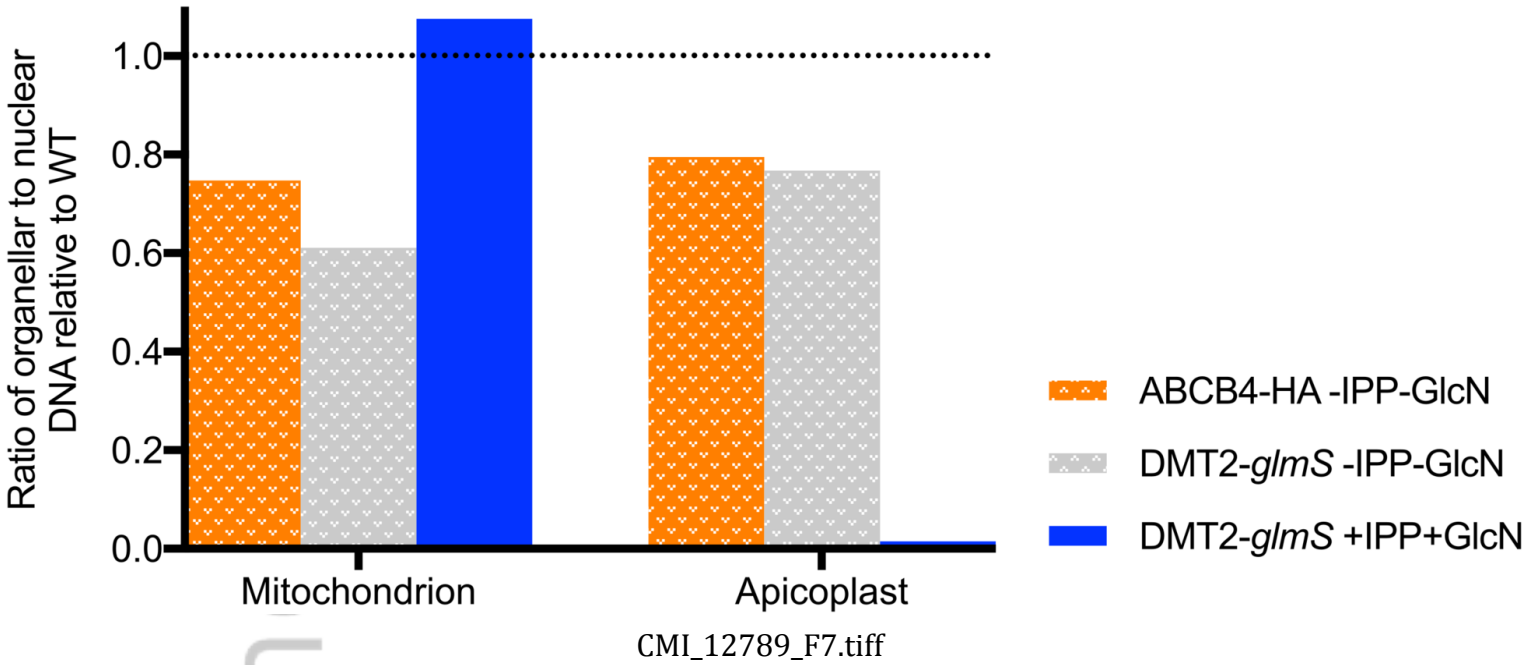


CMI_12789_F7.tiff

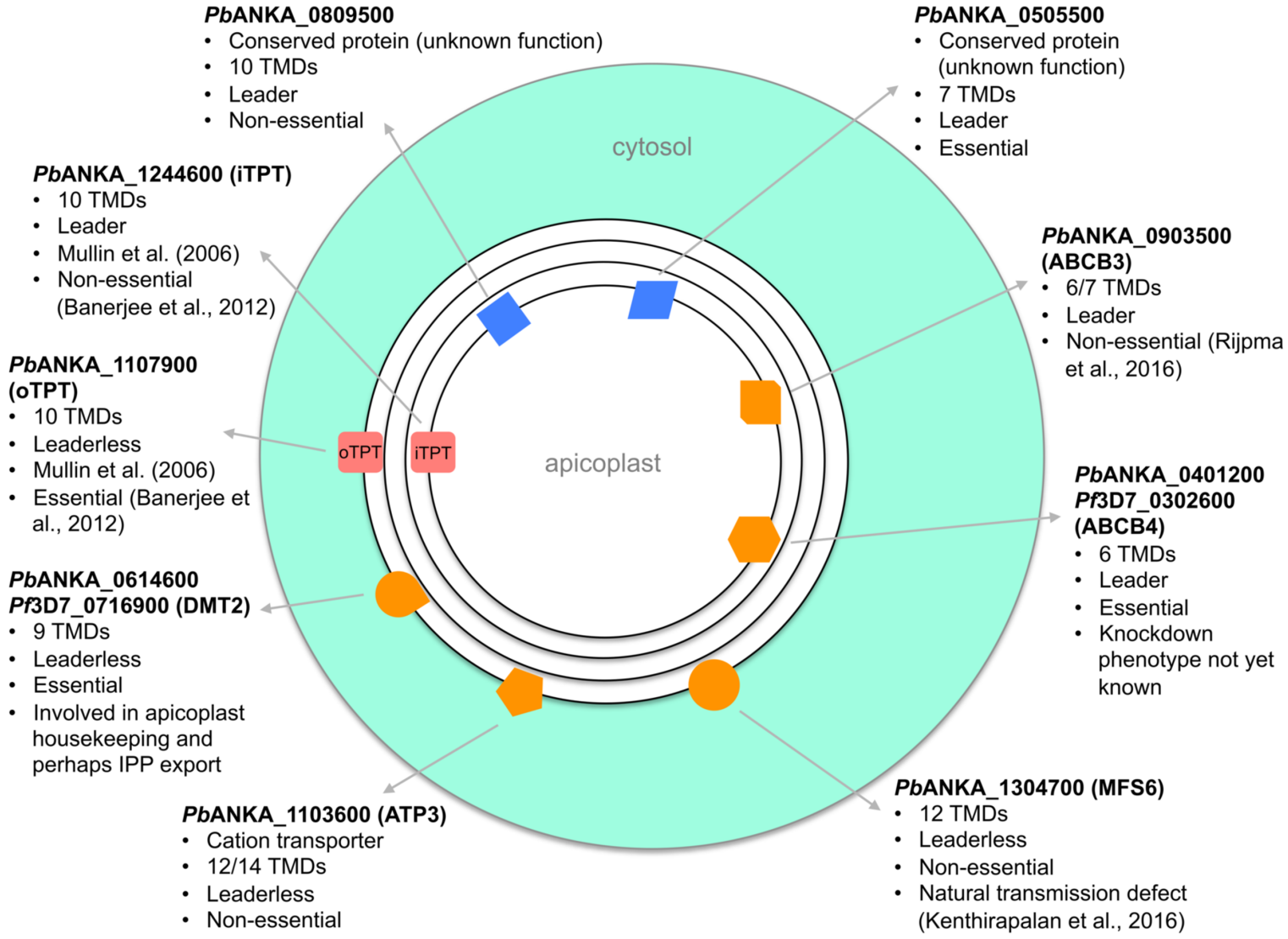


CMI_12789_F8.tiff